C.P. No. 1377

C.P. No. 1377

PROCUREMENT EXECUTIVE, MINISTRY OF DEFENCE

AERONAUTICAL RESEARCH COUNCIL

CURRENT PAPERS

The Calibration of Injector-Powered Engine Simulators for Use in Pressurised Wind Tunnels

by

*A. Masson***

and

D. N. Foster

Aerodynamics Dept., R.A.E., Farnborough Hants.

LONDON: HER MAJESTY'S STATIONERY OFFICE

1977

£2-50 NET

UDC 533.6.072 : 621.438 : 533.6.071.4 : 621.694.2

*CP No.1377
February, 1976

THE CALIBRATION OF INJECTOR-POWERED ENGINE SIMULATORS FOR USE IN PRESSURISED WIND TUNNELS

by

A. Masson**
D. N. Foster†

SUMMARY

The use of engine simulators based on the injector principle is of interest to both ONERA and RAE for use in their respective low-speed pressurised wind tunnels which are currently under construction. As a result of this common interest, a collaborative programme of work was undertaken within the framework of AFARP 1 (Anglo-French Aeronautical Research Programme).

The possibility of using the S3 wind tunnel at Modane-Avrieux to calibrate injector-powered engine simulators was investigated by ONERA using two engine simulators; one built by ONERA to simulate an engine with a by-pass ratio of 10 (M45S), and one built by RAE to simulate an engine with a by-pass ratio of 5 (RB 211). Tests were carried out over a range of stagnation pressures of both the primary (inducing) flow and of the external (induced) flow, under static and low forward speed conditions, with the models at zero angle of incidence. The tests showed that it would be possible to use the S3 wind tunnel to calibrate future engine simulators, and also that, for the conditions tested, the stagnation pressure of the induced flow had only a minimal effect on the non-dimensional performance of the engine simulator.

A description is also given of the tests made in a specially-designed static rig to develop the configuration of the primary nozzles for the ONERA model engine.

---

* Replaces RAE Technical Report 76018 - ARC 36787

** Office National D'Etudes et de Recherches Aerospatiales, Modane-Avrieux, France.

† Royal Aircraft Establishment, Bedford, England.

CONTENTS

1 INTRODUCTION

It is probable that in the future testing of aircraft models in low-speed wind tunnels greater emphasis will be placed on the need to simulate the flow associated with the engines of the aircraft. This need arises in part from the aircraft configurations being proposed to meet the requirement to reduce the noise generated by aircraft. In addition to treatment of the engine itself, it has been suggested that further reductions of noise can be achieved if parts of the airframe are used to shield that part of the engine and efflux noise that would normally be radiated to the ground. As a result the aircraft layout is somewhat unconventional, and interference could result between the intake flow and the wing, if this is used to shield the forward propagating noise, and between the efflux and the tailplane, if this is used to shield the efflux noise. There will then be a need to simulate both the intake and the efflux flows of the engine. A second area of need arises from interest in short field performance and in descent at steep angles. These two aspects of aircraft performance require that the aircraft generates a high lift coefficient, which can be greater than that achievable naturally using slotted leading- and trailing-edge devices. It may then be necessary to utilize the favourable interaction between the efflux of the propulsion engines and the circulation around the wing, as in the external-flow jet-flap scheme. In tests of such schemes it is essential that at least the efflux of the engines be simulated in the wind tunnel.

At RAE, the development of specific units to simulate engines began with units to simulate jet-lift engines[1], and continued with the development of models of propulsion engines[2]. The units were based on the injector principle, as it had been shown[1] that an injector unit driven by cold compressed air may, in fact, be able to simulate both the intake flow coefficient and the exit momentum coefficient of a real engine operating with a cold intake flow and a hot efflux. The injector unit thus allows the effect of intake flows as well as efflux flows to be simulated; even if simulation of the intake flow is not considered necessary, the injector requires a smaller flow of high pressure air than a system involving direct simulation of the efflux flow, and so the problems of passing the air around the wind tunnel balance are simplified. ONERA are currently constructing a rig, designed for the large wind tunnel at Modane-Avrieux (S1)[3], capable of operating at both low and transonic speeds, to study the aerodynamic characteristics of STOL aircraft under both static and dynamic conditions. The models tested on this rig will require the simulation of the engine flow, and

ONERA has already built an injector-powered model which simulates the M45S, an engine having a by-pass ratio of 10.

A number of injector-powered engine simulation units have thus been developed to operate effectively in atmospheric, or sub-atmospheric, wind tunnels. However in the near future RAE and ONERA will each possess a pressurised low-speed wind tunnel. The RAE tunnel, with a working section 5m × 4.2m, will be capable of being pressurised to 3 bars. Intended primarily for the testing of models of aircraft designed for conventional airfield lengths, it will nevertheless be used for testing models of STOL aircraft, and consideration has been given to the nature of the engine simulators that will be used. The F1 Fauga wind tunnel, with a working section 4.5m × 3.5m, will provide ONERA with a wind tunnel capable of being pressurised to 4 bars.

In their contribution to the discussions of the Large Wind Tunnels Working Group, Melzer and Wulf[4] have noted that, in principle, there are no reasons why injector units cannot be used in a pressurised tunnel. They point out, however, that to derive accurate aerodynamic data from model tests in the pressurised tunnel, calibration measurements will have to be performed on the model engine at the same pressure level, and, if these calibration tests are not to incur the high cost resulting from the use of the large pressurised wind tunnel, an adequate small pressurised tunnel is needed. It is possible that the S3 wind tunnel at Modane-Avrieux could fulfil this role. After discussions within the Anglo-French Aeronautical Research Programme (AFARP 1), ONERA undertook a series of tests in this wind tunnel with two model engines, their own model of the M45S and a model supplied by RAE, to explore the use of this facility as a calibration wind tunnel, and to determine the effect of pressurisation on the performance of the model engine.

2 THE MODEL ENGINES

Figs.1 and 2 show the two model engines mounted in the ONERA S3MA wind tunnel. The RAE model was designed by Crane[2], and is designated RAE model 584. It is a model, to approximately 1/20 scale, of an early Rolls-Royce RB 211 engine, having a by-pass ratio of the order of 5.0. A section through the model is given on Fig.3. The 'generator' and 'by-pass' flows were simulated separately, but the primary nozzles for the two flows were fed from a common source of high-pressure air. To ensure that the dimensions of the primary nozzles did not vary as the internal air pressure was increased they were designed as a series

of small circular orifices. In the 'by-pass' flow there were 96 holes of 1.1mm diameter in a ring around the outer wall of the duct, 70 holes of 1.1mm diameter in a ring around the inner wall of the duct, and 64 holes of 1.55mm diameter at the trailing edges of struts extending radially across the duct. In the 'generator' flow there were 39 holes of 1.05mm diameter in a ring around the outer wall of the duct, and 20 holes of 1.75mm diameter at the trailing edges of struts extending radially inwards from the outer wall of the duct.

The ONERA model engine was designed as a 1/10 scale model of the SNECMA M45S engine. This engine, which was a joint project between SNECMA and Rolls-Royce for a turbofan engine with a variable pitch fan, was also known as the RB 410. It was derived from the M45H, an existing engine having a by-pass ratio of 2.85, by the replacement of the fixed fan of this engine with a variable pitch fan, which increased the by-pass ratio to about 10. Fig.2 shows the model modified to simulate a version of the engine recently proposed, and designated M45S D-02 (RB 410-02), in which the 'generator' duct has been extended rearwards to accommodate an extra turbine stage, and to allow the installation of sound-absorbing material.

Fig.4 shows a section through the ONERA model engine, and includes both the M45S and M45S D versions. The 'generator' and 'by-pass' flows are again simulated separately, and the primary nozzles in the two flows are fed from separate and independently-controlled air supplies*. The form of the primary nozzles to provide the highest possible entrainment coefficient (induced mass-flow/primary massflow) was the subject of extensive development work in a specially-designed static rig, and this work is described in Appendix A. In the version tested in the S3MA wind tunnel, the primary nozzles of the 'by-pass' flow were in the form of rectangular slots at the trailing edges of struts extending radially outwards from the inner wall of the 'by-pass' duct. There were nine slots measuring 32mm × 1.5mm, six slots 25mm × 0.5mm, and two slots, within the supporting struts B and C, of 25mm × 0.5mm. In the 'generator' flow the primary nozzle was in the form of an annular slot 2mm wide in the centre body.

Both models were equipped with instrumentation to measure the total and static pressure of the intake and exit flows. In the RAE model engine, Fig.3,

---

* The primary nozzles of the 'generator' and 'by-pass' flows were fed from separate air supplies only for the development tests under static conditions described in Appendix A. For the final version tested in the S3MA wind tunnel, both sets of primary nozzles were fed from a single source of high-pressure air.

single measurements of the total pressure in the flow, and of the static pressure on the duct wall, were possible, together with some measurements of the static pressure on the outside of the cowls. The pressure and temperature of the primary air was also measured. In the ONERA model, Fig.4, the total and static pressure distributions across the flows were measured by rakes installed in the intake, and at the exit planes of the 'generator' and 'by-pass' flows. The total and static pressures of the individual primary flows were also measured. Table 1 lists the quantities measured in the two model engines.

3 THE WIND TUNNEL, BALANCE AND TEST ARRANGEMENTS

3.1 The wind tunnel

The S3 wind tunnel at Modane[5], Fig.5, has a working section 0.78m × 0.56m, and was designed as a blow-down wind tunnel with interchangeable nozzles, allowing tests at subsonic and transonic speeds up to M = 1.35, and fixed supersonic Mach numbers, 2, 3.4 and 4.5. The pressure in the working section can be raised to 4 bar, and the compressed air for the tunnel is stored in six spherical reservoirs with a total capacity of 5500m^3 (five reservoirs of 1000m^3 and one of 500m^3 immediately upstream of the wind tunnel). Depending on the requirements of the tests some or all of these reservoirs are used; certain of these can also be used as vacuum reservoirs connected to the downstream end of the wind tunnel when a Mach number greater than 3.4 is required. For the tests of the model engines the normal transonic working section was used. This working section has perforated sides, the vertical walls having 30% open area and the roof and floor having 9.7% open area. The vertical walls were fitted with turntables; that in the port wall contained a glass panel, whilst that in the starboard wall carried the balance.

3.2 Installation of the models in the wind tunnel

The models were mounted on a common supporting strut from the starboard turntable of the wind tunnel. This type of installation effectively limited the tests to zero angle of incidence. Although the turntable would allow the angle of incidence of the model to be altered the resultant configuration is aerodynamically incorrect; a change of angle of incidence of the model is accompanied by a change of angle of incidence of the strut, which is not representative of the situation on a real aircraft. To test the model at an angle of incidence, or in the presence of a wing, alternative installations must be devised. One such installation, shown on Fig.6, uses the sting rig of this wind tunnel.

3.3 Balance

The balance employed in these tests was that frequently used for tests of helicopter rotors, and referred to as 'triangular-plate balance No.1 (version 3)'. The balance consists of two plates of triangular planform (one fixed and one live and carrying the model), connected by six dynamometers. Three dynamometers (N_1, N_2 and N_3, Fig.7) with a nominal capacity of 2500N, basically measure lift, drag and pitching moment, whilst the remaining three dynamometers, Z_1, Z_2 and Z_3, with a nominal capacity of 15000N, basically measure sideforce, rolling moment and yawing moment. The dynamometers N_1, N_2 and N_3 are fitted with platinum-tungsten strain gauges (350 ohms) and are connected to an 8 volt supply for these tests; the dynamometers Z_1, Z_2 and Z_3 are fitted with Constantin strain gauges having a resistance of 120 ohms, and are connected to a 4 volt supply. The strain gauges were connected to a Wheatstone's bridge, and two sets of bridges are mounted independently on each dynamometer as an insurance against the failure of a gauge.

The balance was mounted on the starboard turntable of the wind tunnel, within a fairing which ensured that the pressure around the balance was the same as that in the working section of the wind tunnel. For this application, the mounting of the balance was modified to allow the passage of air between the plates (fixed and live) of the balance. The air passed through metallic bellows designed to minimise the effect of air pressure on the measurements. A calibration of the balance under these conditions has shown that the air pressure had no effect on the sensitivities of the dynamometers, but resulted in a shift of the zero. This effect was allowed for in the reduction of the results.

3.4 Air supply system

The air supply system[6] was based on a reservoir which is a sphere of $1m^3$ volume. The reservoir incorporates a system to regulate the air pressure, and is connected to three pipelines, known as the primary, secondary and tertiary flows. Each of these pipelines incorporates a system for measuring the massflow of compressed air which includes a sonic nozzle which is removable and interchangeable. For the primary circuit there are three circular nozzles with throat diameters of 45mm, 32mm, and 16mm. As the pressure in the sphere may be controlled over the full range from 7 to 55 bars, the three nozzles can measure respectively 2.5 to 20kg/s; 1.25 to 10kg/s and 0.625 to 5kg/s. Pressures are measured in the sphere (p_{sph}), at the wall of the pipe upstream of the nozzle (p_d) and on the downstream face of the nozzle (control pressure p_8). Temperatures are measured in the sphere (T_{sph}) and upstream of the nozzle (T_d).

For these tests the primary flow pipeline was used when the primary pressure in the engine was above 15 bars, in conjunction with the massflow meter having a throat diameter of 16.00mm. When the primary pressure was less than 15 bars, the secondary flow pipeline was used with a massflow meter having a throat diameter of 12.72mm.

3.5 Jet-survey rake

A rake carrying twenty total pressure tubes and two thermocouples was mounted on the centre-line of the wind tunnel, and its position behind the model engine could be varied. The rake can be seen in Figs.1, 2 and 7.

4 DESCRIPTION OF TEST PROCEDURE

4.1 Operation of the wind tunnel

Although measurements made under static conditions are the simplest to analyse, and provide all the information necessary to define the performance of the injector, it is not possible to carry out such tests over a range of values of the pressure of the air surrounding the injector. This is because the act of raising the pressure inside the working section of the wind tunnel results in a flow through the working section, and because the model engine itself will induce a small but definite flow in the working section when it is operating. In order to measure the effect of the stagnation pressure of the external flow it was, therefore, necessary to carry out tests at low values of the external flow Mach number; in order to define this Mach number accurately, the minimum value was chosen to be 0.08 (25m/s) and the upper limit for the tests discussed here is 0.25 (80m/s). It was, however, possible to remove the wall carrying the model, supporting strut and balance from the working section, and to carry out static tests at the local atmospheric pressure, approximately 0.9 bar at the altitude of Modane-Avrieux, outside the wind tunnel. These results were used to define the static characteristics of the model engines for this value of the external pressure.

The technique for operating the wind tunnel was as follows. The required primary pressure was first established in the model engine. When this pressure was steady the flow in the wind tunnel was started, and when the flow Mach number and stagnation pressure were steady readings were taken. In general three sets of data were taken. If sufficient air then remained in the tunnel reservoir, the Mach number was changed at the same stagnation pressure, and further readings taken. Finally zero values were taken to ascertain if any time-dependent drifts had occurred.

4.2 Data acquisition

The configuration of the data recording system of the S3MA wind tunnel enabled all the required quantities to be measured in about eleven seconds. This time was effectively determined by the speed of operation of the scanivalves, which had been set to give accurate measurements of pressure. The following quantities were measured:

4.2.1 Tunnel reference parameters

The flow stagnation pressure and stagnation temperature, and the static pressure in the working section, were recorded. The stagnation pressure was measured in the settling chamber by a transducer with a range of 350000Pa (50psi); the difference between the pressure just ahead of the working section and that in the settling chamber was measured by a transducer with a range of 35000Pa (5psi), whilst the stagnation temperature was measured in the settling chamber by a chromel-alumel thermocouple with a cold junction maintained at $0^{o}C$ by an electronic regulator.

4.2.2 Parameters of the high pressure air system

The quantities from which the performance of the high pressure air system was derived were the pressure and temperature of the air in the storage vessel, the pressures upstream and downstream of the massflow meter, and the temperature of the air at the massflow meter. The pressure of the air in the storage vessel, and that upstream of the massflow meter, were measured by capsules with ranges of 3 bar, against absolute reference pressures. The pressure downstream of the massflow meter was measured by a capsule with a range of 50 bars, against atmospheric pressure, whilst the temperatures in the sphere and the massflow meter were measured by chromel-alumel thermocouples whose cold junctions were maintained at constant temperature in an oil bath, the temperature of the latter being measured by a mercury thermometer.

4.2.3 Balance output

The signals from the strain gauges mounted on the six dynamometers on the balance were recorded in mV.

4.2.4 Parameters measured on the model

All the pressures to be measured on the model and the twenty pressures to be measured on the jet-survey rake were connected to a D-type scanivalve fitted with a transducer having a range of 350000Pa (50psi) or of 105000Pa (15psi)

depending on the pressure in the wind tunnel. The reference pressure for the transducer was maintained constant at atmospheric pressure plus 60000Pa. The latter pressure was measured by a 'Baudouin' master gauge.

The primary injection pressure was measured by a Bell and Howell gauge with a range of 35 bars (500psi) against atmospheric pressure.

The temperatures T_1 and T_2 on the rake, and the temperatures T_{j1} and T_{j2} inside the RAE model, were measured by chromel-alumel thermocouples whose cold junctions were maintained at constant temperature in an oil bath, the temperature of the latter being measured by a mercury thermometer.

5 REDUCTION OF RESULTS

Three computer programs were used in the reduction of the results at Modane-Avrieux. The first, program 133.250, derived the forces and moments from the balance readings, evaluated the main parameters of the flow in the wind tunnel from the measurements of pressures and temperatures, and produced non-dimensional coefficients from the balance loads. The second program, program 325.251, calculated the pressures measured by the scanivalve. The third program calculated the flow velocities and massflows from the pressure measurements made within the model.

The intake velocity was calculated from the total and static pressures measured at the intake and the stagnation temperature of the wind-tunnel airstream. The velocity distribution in the jet was calculated using the static pressure of the wind-tunnel airstream, and the total pressures and stagnation temperatures measured by the jet-survey rake.

The values of the axial force derived from the balance measurements for model 584 were then corrected to allow for the skin friction force on the cowl of the 'by-pass' flow, and on the exposed area of the strut, that is the area between the joint line and the model engine, Fig.7. The drag of the exposed surface was assumed to be equal to the drag of a flat plate of the same area, with a turbulent boundary layer from the leading edge of the plate. The corrections, obtained using the Royal Aeronautical Society data sheets[7], were normally of the same order as the experimental accuracy.

Allowance was also made for the blockage effect of the flow into the intake, and for the flow entrained by the jet, following the method of Ashill[8]. As a result the external flow Mach number was reduced by up to 3%.

It was found that a number of measurements was made with virtually identical values of the primary and external flow stagnation pressures. The values of the thrust suggested that the balance could measure to an accuracy of ±1.0N.

6 DISCUSSION OF RESULTS

6.1 Primary massflow

The primary massflow Q_p is defined as the total flow of high-pressure air through the primary nozzles of the 'by-pass' and 'generator' flows. For both the RAE model 584 and the ONERA model the high-pressure air is fed into the primary nozzles of both flows at the pressure p_{01}. The primary massflow is presented on Fig.8 as the coefficient $Q_p\sqrt{T_{j1}}/p_{02}A_4$, where p_{02} is the stagnation pressure of the flow external to the engine simulator, and A_4 is the total exit area of the engine ($= A_f + A_g$). It can be seen that the results for the RAE model 584, shown on Fig.8, indicate a linear relationship between this coefficient and the primary pressure ratio, that is the ratio of the stagnation pressure of the primary flow to that of the external flow, p_{01}/p_{02}. Measurements for the ONERA model indicate a similar relationship.

The theoretical relationship between this coefficient and the primary pressure ratio, for the flow of an inviscid gas through a nozzle having a throat area equal to the area of the primary nozzles, is also included on this figure. A comparison of the two lines suggests that the effective throat area of the primary nozzles is less than the geometric area, and gives a value of the discharge coefficient C_D, defined as the ratio of the measured to the theoretical massflow, of 0.865.

6.2 Intake massflow

The intake massflow is shown on Fig.9 as a non-dimensional coefficient, which represents the ratio of the massflow of air through the intake to the massflow of free-stream air through an area equal to the cross-sectional area of the intake. It can also be considered as the ratio of the cross-sectional area of the intake stream tube far upstream from the model to that at the intake.

The effect of the Mach number of the external flow on this coefficient is shown on Fig.9 for the two models. For the range of Mach numbers being considered the coefficient varies in a similar manner for both models: a continuous reduction of the coefficient to the order of unity at a Mach number of 0.25. The figure also shows that the modification of the shape of the 'generator' duct to

simulate the M45S D version of the ONERA model has little effect on the results, and suggests that the geometric characteristics of the model have only a small effect on the coefficient. On the other hand variation of the primary and secondary pressure, at a given Mach number, would enable the value of the coefficient to be adjusted to match that of a real engine.

6.3 Entrainment coefficient

The entrainment coefficient is the ratio of the intake massflow to the primary massflow. Fig.10 shows the effect of primary pressure ratio on this coefficient, and includes results measured under static conditions, with the model removed from the wind tunnel, and under quasi-static conditions, with the model installed in the wind tunnel. As might be expected, the entrainment coefficient falls with increasing pressure ratio. At all values of the primary pressure ratio, a change of Mach number (within the range being considered here) did not affect the coefficient.

6.4 Momentum flow

The momentum flow of the air entering or leaving the engine simulator may be evaluated from the pressures measured in the model. The exit momentum flow may be non-dimensionalised by dividing by the product $p_{02}A_4$, as above, to give a coefficient

$$C\mu = \frac{(\rho AV^2)_f + (\rho AV^2)_g}{p_{02}A_4} .$$

Fig.11 shows the variation of this coefficient with the primary pressure ratio for the two models, for the tests carried out under static and quasi-static conditions. The curve for the RAE model suggests that the rate of increase of the momentum flow coefficient with primary pressure ratio is lower for values of the primary pressure ratio in the range 10 to 14 than at lower or higher values of the primary pressure ratio. This probably results from the distribution of velocity in the efflux varying with the primary pressure ratio, so that the single total and static pressures measured at the exits of the 'generator' and 'by-pass' ducts do not always represent the true mean total and static pressures.

In contrast the exit momentum coefficient measured under static conditions for the ONERA model shows a smooth variation with primary pressure ratio,

although no measurements were made for a primary pressure ratio greater than 14. This probably reflects the fact that the velocities used in the evaluation of this coefficient were mean values derived from the total and static pressure rakes installed in the 'by-pass' and 'generator' ducts. Measurements made under forward speed conditions show, in a similar manner to the entrainment coefficient, that at a given Mach number the exit momentum coefficient is dependent on the primary pressure ratio, so that any value required to simulate the performance of a real engine can be achieved by variation of the primary pressure ratio.

6.5 Flow velocities measured at jet-survey rake

Velocity distributions in the jets downstream of the model engines were measured using the rake of twenty total pressure tubes. In addition, the ONERA model was equipped with total pressure rakes at the exits of the 'generator' and 'by-pass' ducts.

Measurements made with the jet-survey rake at different distances downstream of the model showed that the velocity distributions in the jet, and the growth of the jet, were hardly affected by the presence of an external flow. The results also showed that the velocity distributions measured for different values of the primary pressure ratio were similar. Fig.12 shows results for the RAE model under static conditions for different primary pressure ratios, the velocities having been made non-dimensional by dividing by the maximum velocity in the jet, taken as being equal to that measured on tube No.10. The results obtained under forward speed conditions also showed similar velocity distributions, the velocity at any point in the jet being increased from the static value simply by the external flow velocity.

Fig.13 shows the development of the velocity distribution in the jet downstream of the two models. The results were measured under static conditions for the ONERA model, and for a low external-flow velocity for the RAE model. In both cases, the jet is diverging as a cone with a semi-angle of 4°. The measurements were made within the length of the 'potential core' of the jet, and so it is not surprising that this angle is less than the value of 6.2° which would be predicted for the expansion of a single jet downstream of the 'potential core' by the equations given by Küchemann and Weber[9]. The shape of the expanding double-jet will also be affected by the presence of the cowl of the 'generator' flow.

The figure also shows that two different velocity distributions were measured at the exit of the 'by-pass' flow of the ONERA model. In fact, these

two types of velocity profiles are present alternately around the circumference of the jet, depending on whether the measurements were made in the flow from an injector slot or not. The length of duct in which the injected air and the induced air can mix is not sufficient for complete mixing, and the injected air is still identifiable at the exit of the 'by-pass' flow. Fig.13 shows that mixing of the flow occurs rapidly downstream of the exit of the engine,so that no changes are required within the engine to increase the rate of mixing in the 'by-pass' flow.

A survey of the available measurements of flow velocity made for full-scale engines failed to reveal any data corresponding to Fig.13. However the National Gas Turbine Establishment had measured the variation of total pressure across the 'by-pass' duct of a full-scale RB 211 engine near to the exit of the duct at low forward speeds. From these measurements Fig.14 has been derived, assuming that the local static pressure was equal to the static pressure of the external flow. Some variation of the distribution around the duct is evident, but the results suggest that the most appropriate velocity distribution for the injector-powered engine simulator would be one with a constant velocity across the duct, with, perhaps, some fall-off close to the duct walls.

6.6 Measurements of net thrust

The analysis of Appendix B suggests that a non-dimensional thrust coefficient C_T will, for a given injector, depend only on the primary pressure ratio p_{01}/p_{02}, and the external flow Mach number M_∞. This presentation has been used in Figs.15 and 16, where it can be seen that the experimental thrust coefficient for the RAE model increases with the pressure ratio less rapidly than that indicated by the theoretical predictions. These predictions are for a simplified injector which has the same value of the ratio of the area of the final mixed flow duct to the area of the primary nozzle as the real injector, and which operates in an inviscid fluid.

Figs.17 and 18 show the variation of the thrust coefficient with the external flow Mach number, for two values of the primary pressure ratio, and a range of external pressures. Both figures suggest that the external pressure has only a small effect on the thrust coefficient. However as is inevitable in experimental work, the value of the primary pressure ratio was not precisely the same for each of the points shown on the respective figures, and, as Figs.15 and 16 show, the thrust coefficient is strongly dependent on the primary pressure ratio. In order, therefore, to consider the effect of external pressure

independently from changes of the primary pressure ratio, the measured values of the thrust coefficient have been divided by the theoretical value of the thrust coefficient for the simplified injector, calculated for the measured primary pressure ratio and the Mach number of the external flow. Fig.19 suggests that this ratio increases slightly with increase of external pressure. For the results at a primary pressure ratio of approximately 10.0, the maximum increase of thrust on increasing the external pressure, as indicated by the points, represents 0.9% of the thrust. However the scatter of the balance readings referred to earlier could account for a difference of 0.4% of the thrust. Thus at this value of the primary pressure ratio, the effect of the external pressure may represent only 0.5% of the thrust. At the primary pressure ratio of approximately 5.0, the maximum change of thrust indicated by the points is somewhat larger, 2.4%. However the effect of the scatter of the balance readings is also larger, due to the lower values of the forces being measured at this value of the primary pressure ratio, and could account for a difference of 1.0% of the thrust. Thus the effect of the external pressure may, at this primary pressure ratio, represent only 1.4% of the thrust.

The concept of the ratio of the experimental thrust coefficient to the theoretical thrust coefficient as a measure of the efficiency of the injector has been extended in Fig.20 to highlight the factors affecting the thrust efficiency. Compared with the theoretical performance of the simplified injector, the thrust efficiency is seen to be independent of the external flow Mach number at a given primary pressure ratio, and to increase slowly with the primary pressure ratio. The theoretical model ceases to be valid for primary pressure ratios in excess of 13.4, since it would then predict Mach numbers in the fully mixed flow (M_4) greater than unity. However it can also be seen that the maximum value of the thrust efficiency is only just over 60%, so that a loss of some 40% of the theoretical thrust must be attributed to the detailed differences between the geometry of the simplified and real injector, and to viscous losses in the primary and irduced flow (see Appendix B).

In the simplified injector, it is assumed that the primary flow is injected through a single nozzle whose walls are of negligible thickness at the plane of the injection of the primary flow. In the real injector, the primary flow is injected through a number of small orifices set in a series of radial struts, and the area of the downstream face of the struts (the 'base area') which surrounds the primary nozzles at the plane of injection reduces the effective

area of the induced flow duct. The theoretical model has been modified to allow for this base area, and as a result the theoretical thrust coefficient has been reduced, and the thrust efficiency increased. Fig.20 indicates that the effect of the base area is greatest at the lower values of the primary pressure ratio, giving an increase in the thrust efficiency of approximately 10%, but at the higher values of the primary pressure ratio the effect of the base area is reduced, and there is the suggestion that at very high values of the primary pressure ratio the curve including allowance for the base area would approach that for the simple injector, and the effect of the base area would then be very small.

The effect of the viscosity of the real fluid is to reduce the effective area of the primary nozzle, so that, as was noted earlier (Fig.8) the massflow through the primary nozzles was only some 86.5% of the theoretical massflow. This value of the nozzle discharge coefficient has been included in the theoretical analysis and, as Fig.20 shows, results in a rather larger increase in the thrust efficiency, this increase being approximately independent of the value of the primary pressure ratio. The thrust efficiency is, however, still less than 100%, and the remaining loss must result from factors not so far included in the analysis. These factors are the viscous losses in the induced flow duct, and pressures on the base area in the induced flow duct. The magnitude of the loss due to these factors is dependent on the value of the primary pressure ratio, but the analysis of the results presented on Fig.19 suggests that it is only very slightly affected by changes of the external pressure; i.e. by changes in the Reynolds number of the induced flow.

7 CONCLUSIONS

The tests conducted on the model engines have shown that, in principle, the S3MA wind tunnel has all the facilities necessary to calibrate injector-powered engine simulators destined for use in pressurised wind tunnels. The accuracy of the measurement of engine thrust is considered to be adequate, as it is equivalent, for a typical STOL model currently being designed to be tested in the pressurised wind tunnels, to an uncertainty of 0.0010 in the measurement of the drag coefficient. Analysis of the tests has shown that when assessing the effect of external pressure on the characteristics of the model engine, account must be taken of the comparatively large effect of slight differences in the value of the primary pressure ratio. When these effects are allowed for, the

results indicate that, for a model engine at zero angle of incidence to the external flow, the non-dimensional performance is only weakly dependent on the total pressure of the external flow.

Any future calibration of a model engine intended for specific tests with an aircraft model must give the characteristics of the engine for the full range of flow conditions in which it will have to operate when attached to the model. Thus the characteristics must be measured in a flow with a uniform inclination to the engine axis, as occurs when the model engine is at a non-zero angle of incidence, or when there is a non-uniform inclination of the flow to the engine axis, as occurs when the model engine is mounted close to a wing with highly deflected flaps. It is possible to change the angle of incidence of the model engine for the existing installation by rotation of the turntable, but the situation is then unrepresentative as the supporting strut is also at an angle of incidence. To overcome this problem a different installation must be envisaged, possibly using the existing sting rig of the wind tunnel. With such an installation the S3MA wind tunnel would be able to undertake the full calibration of an injector-powered model engine.

Appendix A

DEVELOPMENT OF THE CONFIGURATION OF PRIMARY NOZZLES FOR ONERA M45S MODEL

The aim of the static test programme for the M45S model, using the rig shown in Fig.21, was to choose the configuration of the primary nozzles which gave the highest entrainment coefficient (induced massflow/primary massflow). Thus this experiment was basically concerned with the measurement of massflows: massflow of air induced into the intake, and the primary massflow, controlled by the primary pressure p_{01}. Measurements of the flow velocities at the exit planes of the 'by-pass' and 'generator' flow were also made to indicate the degree of mixing achieved by the different arrangements. These velocities were deduced from total pressure measurements made with rakes of tubes installed radially across the exit planes of the flows, and static pressures taken at the same planes on the inside of the corresponding duct. It was possible to vary the angular position of the rakes.

The high pressure air system supplying the primary nozzles was the same as that used to supply the model when it was installed in the wind tunnel, section 3.4, and the primary massflow was measured by a sonic nozzle in the pipeline between the reservoir and the model. At the model the pressure of the primary air was measured by a pitot tube in the high-pressure air duct (Fig.4).

The massflow of air induced by the model engine was measured by a venturi made to the standard laid down in NF-X-10-101. In order to install this venturi ahead of the model, a small modification had to be made to the intake of the model, as is shown on Fig.21, the 'Bellmouth'. The massflow was calculated using standard equations, knowing the pressures of the air upstream of the throat, and at the throat, and the temperature of the air upstream of the throat.

As the primary nozzles of the 'generator' and 'by-pass' flows are fed by separate air supplies, it was possible to study the two flows separately or together. The massflow of air induced into the 'generator' duct was measured by a second, smaller venturi (Figs.21 and 22). This venturi was used when the 'generator' flow only was simulated; when the 'by-pass' flow alone was simulated the 'generator' duct was faired over (Fig.22) and the large venturi then measured the flow induced through the 'by-pass' duct. When both flows were being simulated, both venturis were used to enable the individual flow induced into the 'generator' and 'by-pass' ducts to be determined.

Fig.23 shows the results obtained under these circumstances during the study of the configuration of the primary nozzles for the 'by-pass' flow. The effect of the primary pressure p_{01} on the performance of four types of nozzles, including rectangular and circular shapes, is illustrated (the external static pressure was the atmospheric pressure at Modane-Avrieux, $p_{02} \simeq 0.89$ bar). The configuration designated A_2 gave the highest value of the entrainment coefficient m, and was incorporated in the final version of the model which was tested in the wind tunnel.

When this configuration of primary nozzles (or the very similar configuration designated A) was installed in the 'by-pass' flow, the induced massflow Q_{if} varied only slowly with the pressure of the primary air in the range 10 to 15 bars. The characteristics of the injector under these circumstances were then considered to be very close to the optimum characteristics.

Similar results were obtained during the study of the configuration of the primary nozzles for the 'generator' flow. The configuration chosen was an annular slot on a centre body. This configuration results, for a primary pressure of approximately 10 bars, in the complete model engine giving a good simulation of the characteristics of the full-scale engine.

Fig.24 shows the thrust measured for the final model configuration when the model was installed in the wind tunnel, but without any external flow.

Appendix B

ANALYSIS OF FLOW THROUGH INJECTOR TO PREDICT THE NET THRUST

This analysis is based on unpublished work by Lopez at BAC, and Crane at RAE, and work by Wood at RAE[10].

A sketch of the simplified injector, defining the notation, is shown in Fig.25. It will be assumed that the primary and secondary stagnation temperatures T_{01} and T_{02} are equal. Assuming uniform velocity distributions at each station, and ignoring all viscous losses, the continuity and momentum equations for the flow inside the injector are:

$$A_1\rho_1V_1 + A_3\rho_3V_3 = A_4\rho_4V_4 \qquad (1)$$

$$\left(p_1 + \rho_1V_1^2\right)A_1 + \left(p_3 + \rho_3V_3^2\right)A_3 = \left(p_4 + \rho_4V_4^2\right)A_4 \quad . \qquad (2)$$

Dividing throughout by A_2p_4, and using the relationships

$$\frac{p_0}{p} = (1 + 0.2M^2)^{3.5} \qquad \frac{\rho_0}{\rho} = (1 + 0.2M^2)^{2.5}$$

$$\frac{\rho V^2}{p} = 1.4M^2 \qquad \frac{p_0}{\rho_0} = RT_0 = \text{constant}$$

$$AR = \frac{A_4}{A_1} = \frac{A_2}{A_1} \qquad \frac{AR - 1}{AR} = \frac{A_3}{A_2} \quad ,$$

and assuming the primary flow is choked ($M_1 = 1$), equations (1) and (2) reduce to

$$\frac{1}{AR}\frac{p_{01}}{p_4}(1 + 0.2)^{-3} + \frac{AR - 1}{AR}\frac{p_{03}}{p_4}\left(1 + 0.2M_3^2\right)^{-3} = M_4\left(1 + 0.2M_4^2\right)^{\frac{1}{2}} \quad , \qquad (3)$$

and

$$\frac{1}{AR}\frac{p_{01}}{p_4}(1 + 0.2)^{-3.5}(1 + 1.4) + \frac{AR - 1}{AR}\frac{p_{03}}{p_4}\left(1 + 0.2M_3^2\right)^{-3.5}\left(1 + 1.4M_3^2\right)$$

$$= 1 + 1.4M_4^2 \quad . \qquad (4)$$

Assuming further that the exit flow is subsonic, so that $p_4 = p_\infty$, and so

$$\frac{p_{02}}{p_4} = \frac{p_{02}}{p_\infty} = \left(1 + 0.2M_\infty^2\right)^{3.5}$$

with

$$p_{03} = p_{02}$$

equations (3) and (4) become

$$\frac{1}{AR}\frac{p_{01}}{p_{02}}\frac{\left(1 + 0.2M_\infty^2\right)^{3.5}}{(1 + 0.2)^3} + \frac{AR - 1}{AR}\left(1 + 0.2M_\infty^2\right)^{3.5}\frac{M}{\left(1 + 0.2M_3^2\right)^3}$$

$$= M_4\left(1 + 0.2M_4^2\right)^{\frac{1}{2}} \quad , \tag{5}$$

and

$$\frac{1}{AR}\frac{p_{01}}{p_{02}}\frac{\left(1 + 0.2M_\infty^2\right)^{3.5}(1 + 1.4)}{(1 + 0.2)^{3.5}} + \frac{AR - 1}{AR}\left(1 + 0.2M_\infty^2\right)^{3.5}\frac{\left(1 + 1.4M_3^2\right)}{\left(1 + 0.2M_3^2\right)^{3.5}}$$

$$= 1 + 1.4M_4^2 \quad . \tag{6}$$

Thus, given the area ratio AR, the ratio of stagnation pressures p_{01}/p_{02} and the free stream Mach number M_∞, equations (5) and (6) represent two simultaneous equations for the Mach numbers M_3 and M_4. A computer program, written for the Elliott 4130 computer at RAE Bedford, solves these equations using an iterative scheme, starting with equation (5), and putting $M_3 = 0$ to give a value of M_4, and using this value as the initial value of M_3 in equations (5) and (6), subsequently modifying it until the values of M_4 given by the two equations are coincident.

The net thrust of the injector, T, assuming $p_4 = p_\infty$ is given by

$$T = \rho_4 A_4 V_4^2 - \rho_2 V_2 A_2 V_\infty \quad . \tag{7}$$

The mass ratio m is defined as the ratio of secondary to primary flow, so that

$$m = \frac{\rho_2 V_2 A_2}{\rho_1 V_1 A_1} \; ; \qquad \frac{m}{m + 1} = \frac{\rho_2 V_2 A_2}{\rho_4 V_4 A_4} \quad . \tag{8}$$

Hence

$$T = \rho_4 V_4 A_4 \left\{ V_4 - \frac{m}{m + 1} V_\infty \right\} \quad ,$$

or

$$T = \rho_4 a_4 M_4 A_4 \left\{ a_4 M_4 - \frac{m}{m+1} M_\infty a_\infty \right\} \qquad (9)$$

with

$$T_{01} = T_{02} = T_{0\infty} \quad ,$$

$$a_\infty = \left[\frac{1 + 0.2M_4^2}{1 + 0.2M_\infty^2} \right]^{\frac{1}{2}} a_4 \quad .$$

Putting

$$\rho_4 a_4^2 = \rho_4 \frac{1.4p_4}{\rho_4} = 1.4p_4 = \frac{1.4p_{02}}{\left[1 + 0.2M_\infty^2\right]^{3.5}} \quad ,$$

a non-dimensional thrust coefficient may be defined as

$$C_T = \frac{T}{p_{02}A_4} = \frac{1.4M_4}{\left[1 + 0.2M_\infty^2\right]^{3.5}} \left\{ M_4 - \frac{m}{m+1} \left[\frac{1 + 0.2M_4^2}{1 + 0.2M_\infty^2} \right]^{\frac{1}{2}} M_\infty \right\} \quad . \qquad (10)$$

From equations (8) the mass ratio m may be written as

$$m = \frac{\rho_4 V_4 A_4}{\rho_1 V_1 A_1} - 1$$

$$= \left\{ AR \frac{p_{02}}{p_{01}} \frac{(1 + 0.2)^3}{\left(1 + 0.2M_\infty^2\right)^{3.5}} M_4 \left[1 + 0.2M_4^2 \right]^{\frac{1}{2}} \right\} - 1 \quad . \qquad (11)$$

Equations (10) and (11), together with the equations for the mixing process inside the injector, (5) and (6), allow the net thrust of the idealised injector to be calculated. A real injector will differ from the simplified injector analysed above in the following ways:

(i) the construction is in general such that there is an area surrounding the primary nozzles which is not available for the secondary flow. This base area is such that $A_1 + A_3 \neq A_4$;

(ii) viscous effects in the primary nozzles result in the primary massflow being less than the theoretical massflow through the geometric area of the nozzles. The nozzles thus have a discharge coefficient C_D of less than 1.0;

(iii) there are viscous losses in the induced flow along the duct walls, and a base pressure acting on the base area of (i) above.

The theory can be modified for effects (i) and (ii) as follows:

allowing for the discharge coefficient of the primary nozzles C_D, equations (1) and (2) become

$$C_D A_1 \rho_1 V_1 + A_3 \rho_3 V_3 = A_4 \rho_4 V_4 \tag{12}$$

$$C_D \left(p_1 + \rho_1 V_1^2\right) A_1 + \left(p_3 + \rho_3 V_3^2\right) A_3 = \left(p_4 + \rho_4 V_4^2\right) A_4 \tag{13}$$

Defining a new area ratio AR', such that

$$\frac{A_3}{A_4} = \frac{AR' - 1}{AR} \quad ,$$

equations (12) and (13) may be reduced to forms similar to equations (5) and (6), i.e.

$$\frac{C_D}{AR} \frac{p_{01}}{p_{02}} \frac{\left(1 + 0.2M_\infty^2\right)^{3.5}}{(1 + 0.2)^3} + \frac{AR' - 1}{AR'} \left(1 + 0.2M_\infty^2\right)^{3.5} \frac{M_3}{\left(1 + 0.2M_3^2\right)^3}$$

$$= M_4 \left(1 + 0.2M_4^2\right)^{\frac{1}{2}} \tag{14}$$

$$\frac{C_D}{AR} \frac{p_{01}}{p_{02}} \left(1 + 0.2M_\infty^2\right)^{3.5} \frac{(1 + 1.4)}{(1 + 0.2)^{3.5}} + \frac{AR' - 1}{AR'} \left(1 + 0.2M_\infty^2\right)^{3.5} \frac{\left(1 + 1.4M_3^2\right)}{\left(1 + 0.2M_\infty^2\right)^{3.5}}$$

$$= 1 + 1.4M_4^2 \quad . \tag{15}$$

These equations may be solved in the same manner as equations (5) and (6).

The non-dimensional thrust coefficient C_T is again given by equation (10); the mass ratio m is now

$$m = \frac{\rho_2 V_2 A_2}{C_D \rho_1 V_1 A_1}$$

and is given by

$$m = \left\{ \frac{AR}{C_D} \frac{p_{02}}{p_{01}} \frac{(1 + 0.2)^3}{\left(1 + 0.2M_\infty^2\right)^{3.5}} M_4 \left[1 + 0.2M_4^2\right]^{\frac{1}{2}} \right\} - 1 \quad . \tag{16}$$

Table 1

PRESSURE AND TEMPERATURE MEASUREMENTS WITHIN THE MODEL ENGINES

(a) RAE model engine

p_{01}	total pressure of primary air
p_{ti}	total pressure at the intake
p_{si}	static pressure at the intake
p_{tf}, p_{tg}	total pressures at exit of 'by-pass' and 'generator' flows
p_{sf}, p_{sg}	static pressures at exit of 'by-pass' and 'generator' flows
p_{xf}, p_{xg}	static pressures on the outside of 'by-pass' and 'generator' cowls
T_{j1}, T_{j2}	total temperatures of primary air

(b) ONERA model engine

p_{01f}, p_{01g}	total pressures of primary air in 'by-pass' and 'generator' flows
p_f, p_g	static pressures of primary air in 'by-pass' and 'generator' flows
p_{ti} 1-8	total pressures measured on rake in intake
p_{si} 1-8	static pressures measured on rake in intake
p_{pi} 1-5	static pressures measured on inside of intake
p_{i1}, p_{i2}	mean of four static pressures measured at two longitudinal positions in the intake
p_{tf}, p_{tg}	total pressures measured on rakes at exit of 'by-pass' and 'generator' flows
p_{sf}, p_{sg}	mean of four static pressures measured at the exit of the 'by-pass' and 'generator' flows
p_{ssf}, p_{ssm}	mean static pressures measured by traversing a probe across the exit of the 'by-pass' and 'generator' flows

SYMBOLS

A	cross-sectional area
AR	area ratio (Appendix B)
AR'	modified area ratio (Appendix B)
a	speed of sound
C_D	nozzle discharge coefficient
C_T	thrust coefficient
C_μ	momentum flow coefficient
M	Mach number
m	entrainment coefficient (mass ratio)
p	pressure
Q	massflow
T	temperature
T_1, T_2	stagnation temperatures at jet-survey rake
T_{j1}, T_{j2}	stagnation temperatures of primary flow
V	flow velocity
ρ	flow density
ε	intake massflow coefficient

Suffixes

f	relevant to the flow through the 'by-pass' duct
g	relevant to the flow through the 'generator' duct
i	relevant to the intake
j	relevant to the jet
L	local values
p	relevant to the primary flow
∞	relevant to conditions at infinity upstream
0	stagnation conditions
1,2,3,4	relevant to stations in the injector (Fig.25)

REFERENCES

No.	Author	Title, etc.
1	M.N. Wood J.B.W. Howard	The development of injector units for jet-lift engine simulation on low-speed-tunnel models. R & M 3464 (1965)
2	J.F.W. Crane	The design and calibration of a five-inch ejector nacelle simulating an engine of high by-pass ratio. RAE Technical Report in preparation.
3	M. Pierre G. Fasso	Exploitation du centre d'essais aérothermodynamiques de Modane-Avrieux. ONERA NT No.181 (1971)
4	E. Melzer R. Wulf	Use of model engines (V/S/CTOL). Paper No.6 of "Problems in wind tunnel testing techniques". AGARD-R-601 (1973)
5	M. Pierre	Possibilites du centre d'essais aérothermodynamiques de Modane-Avrieux. ONERA NT No.77 (1964)
6	G. Fasso M. Plétin P. Broussaud	Installation pour l'étude de tuyères a plusieurs flux. ONERA NT No.160 (1970)
7	Anon	Royal Aeronautical Society. Data Sheet 68020 (1968)
8	P.R. Ashill	On the blockage interference of a jet-powered model in a wind-tunnel of closed working section. RAE Technical Report in preparation.
9	D. Küchemann J. Weber	Aerodynamics of propulsion. McGraw-Hill, London, pp.237-239 (1953)
10	M.N. Wood	The use of injector units for engine simulation on wind tunnel models at high speeds. RAE Technical Report 71215 (1971)

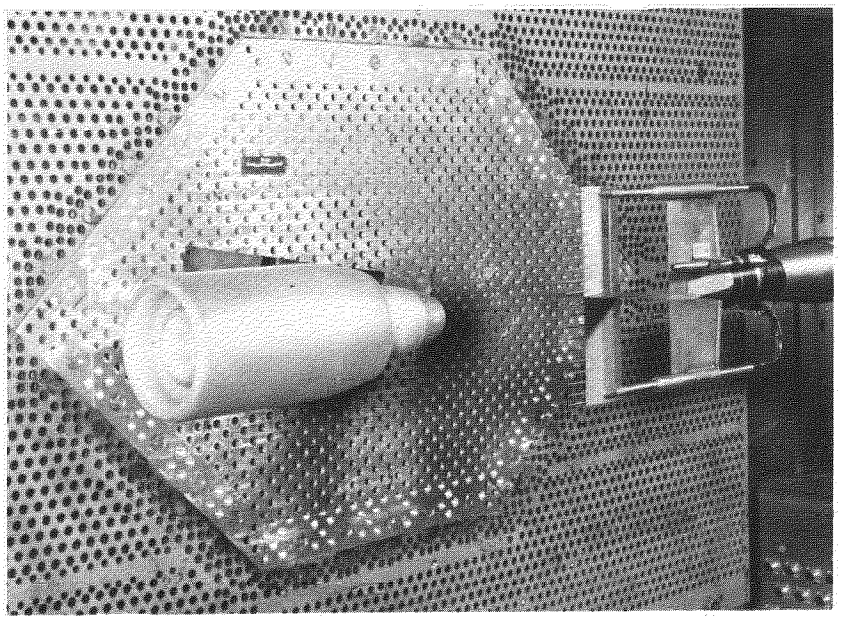

Fig.1 RAE model 584 in S3MA wind tunnel

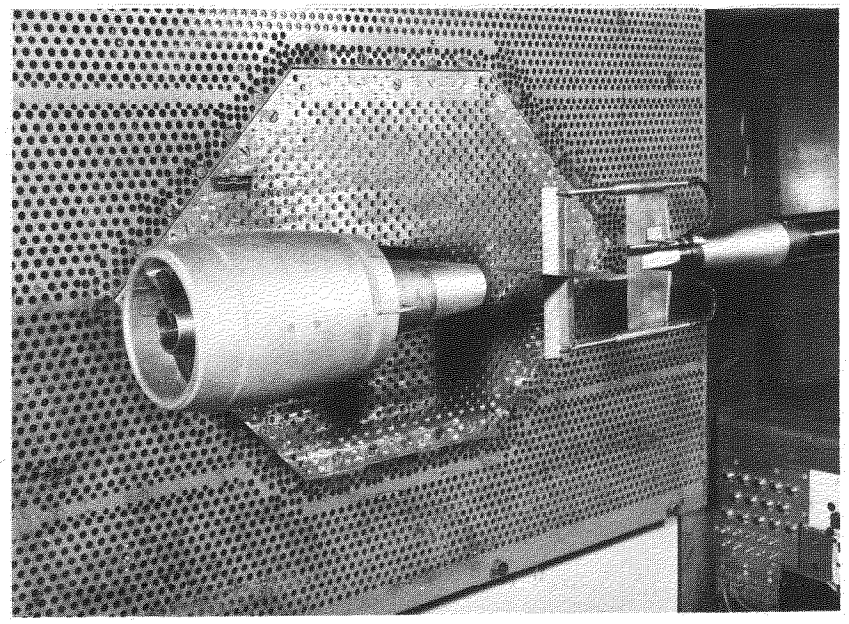

Fig.2 ONERA model M45S D-02 in S3MA wind tunnel

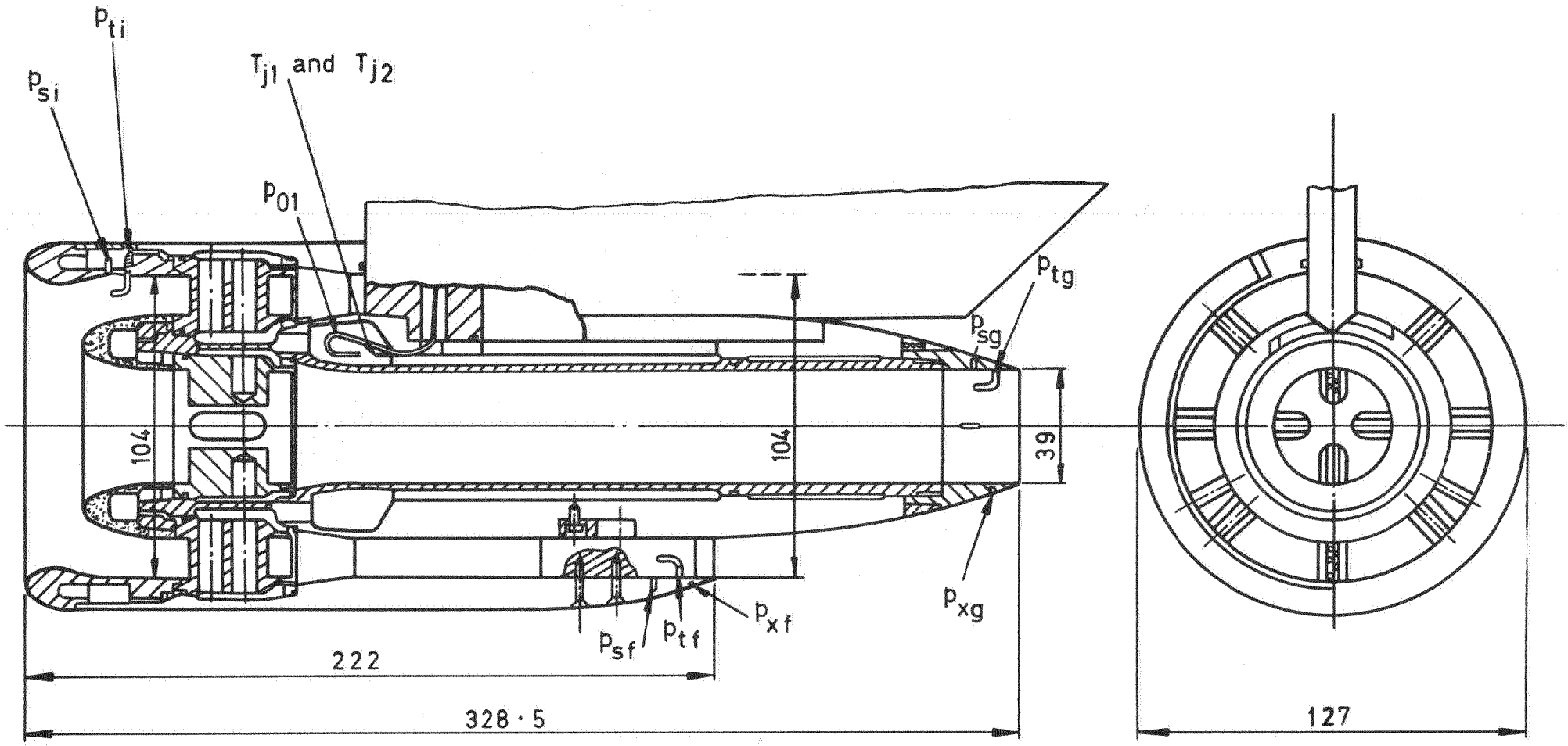

Scale 1:2

Fig.3 RAE model 584

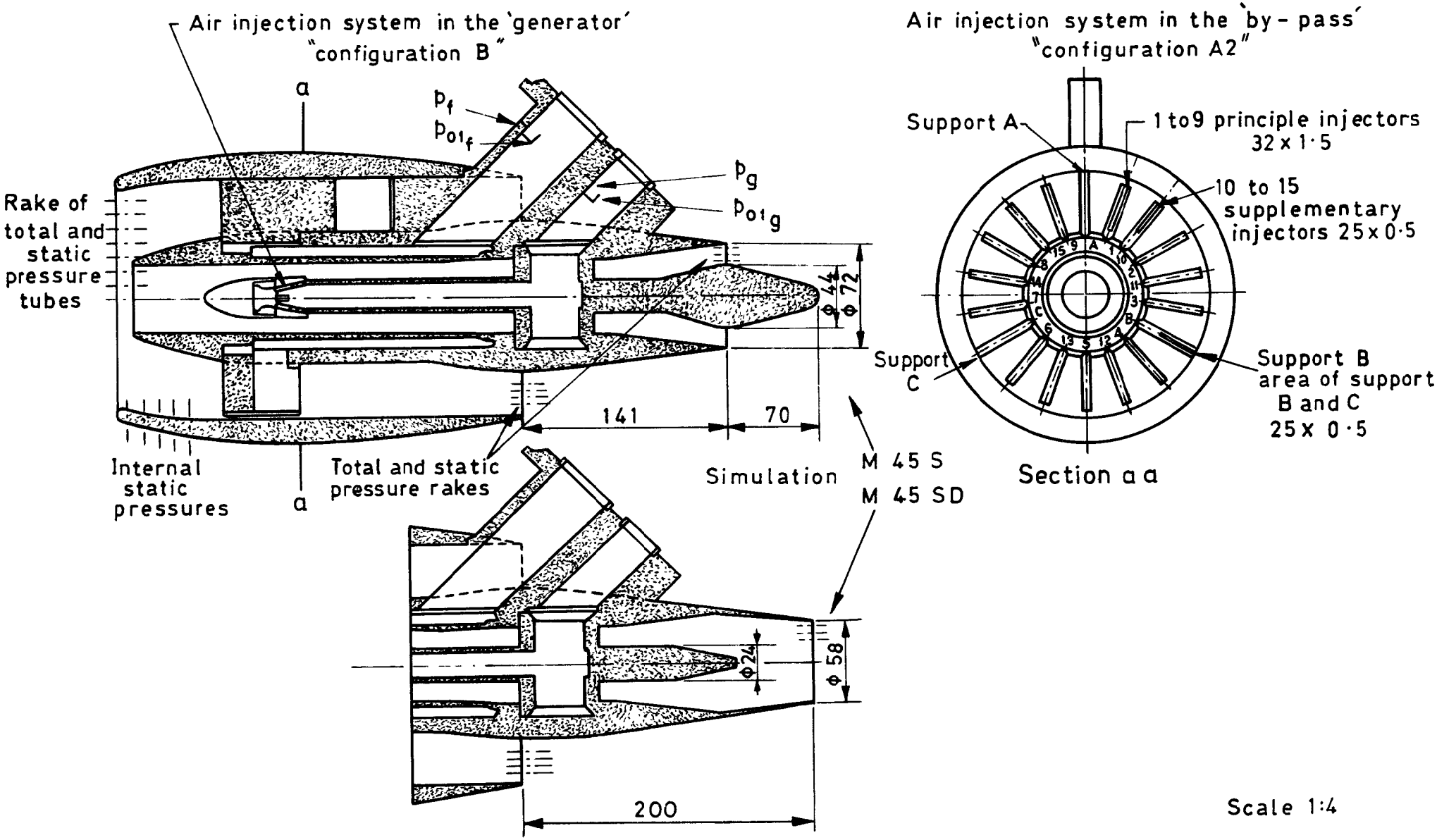

Fig.4 ONERA model M45 S

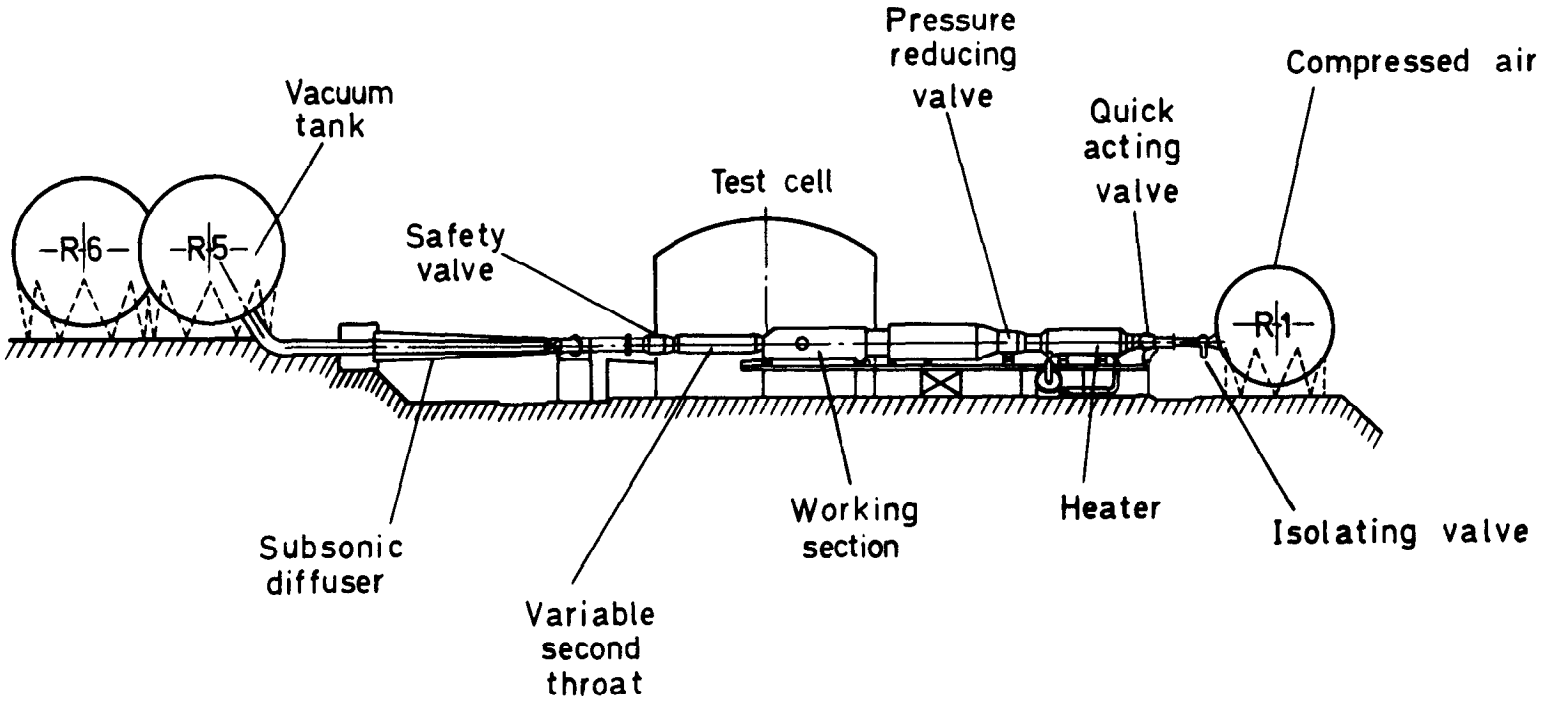

Fig.5 The S3 MA wind tunnel

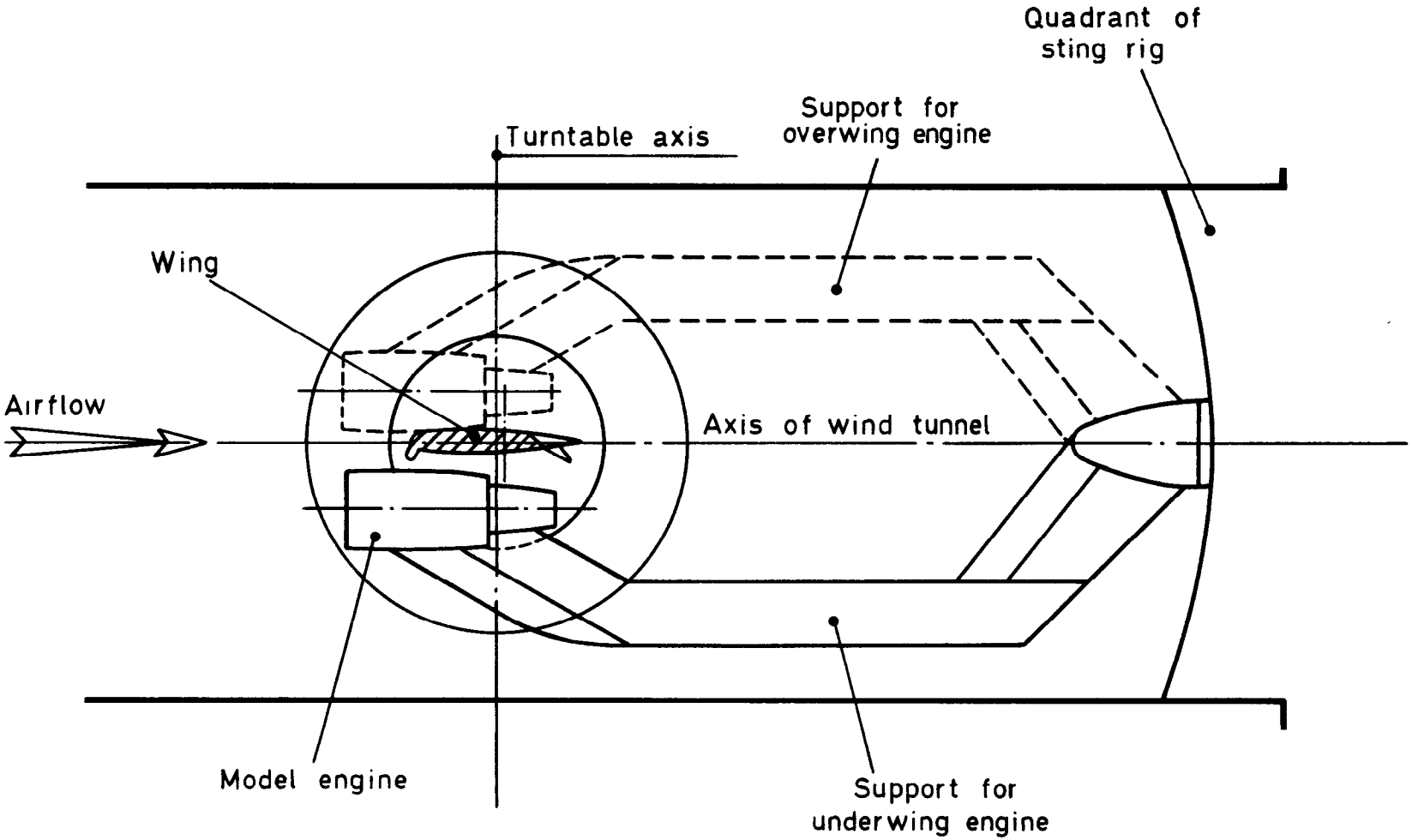

Fig. 6 Possible installation of model in presence of a wing

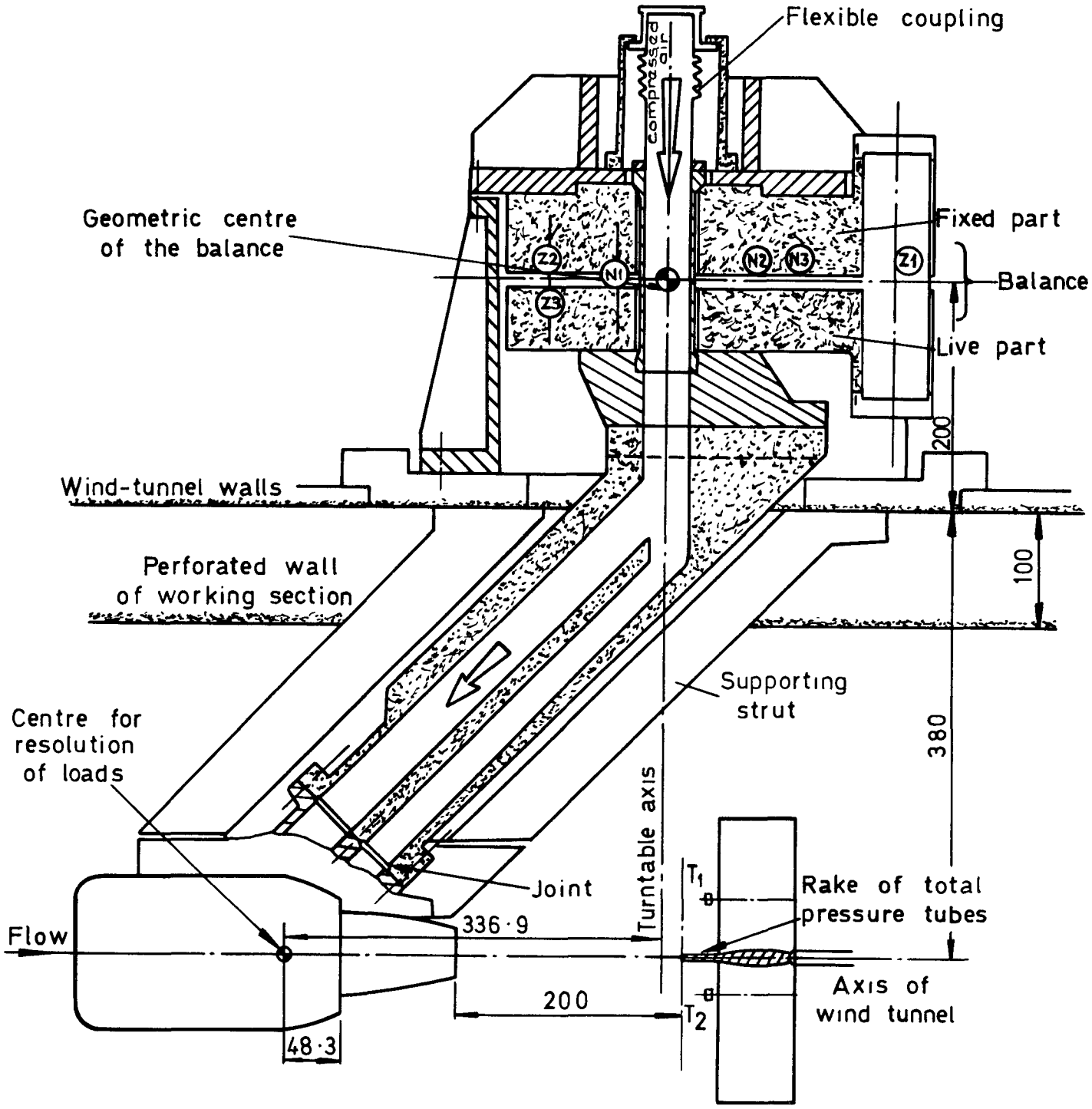

Fig.7 Wind tunnel balance

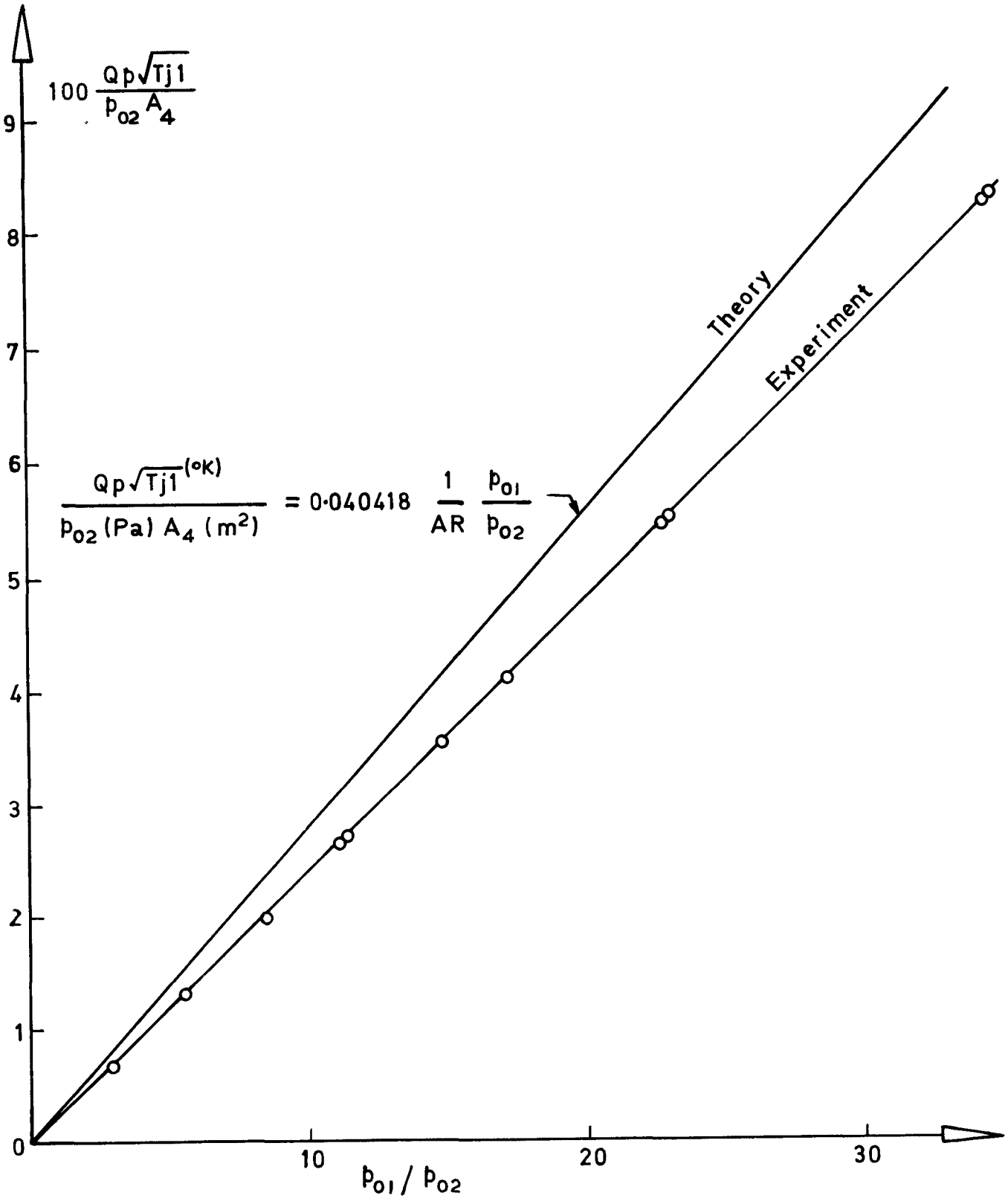

Fig.8 Primary massflow for RAE model

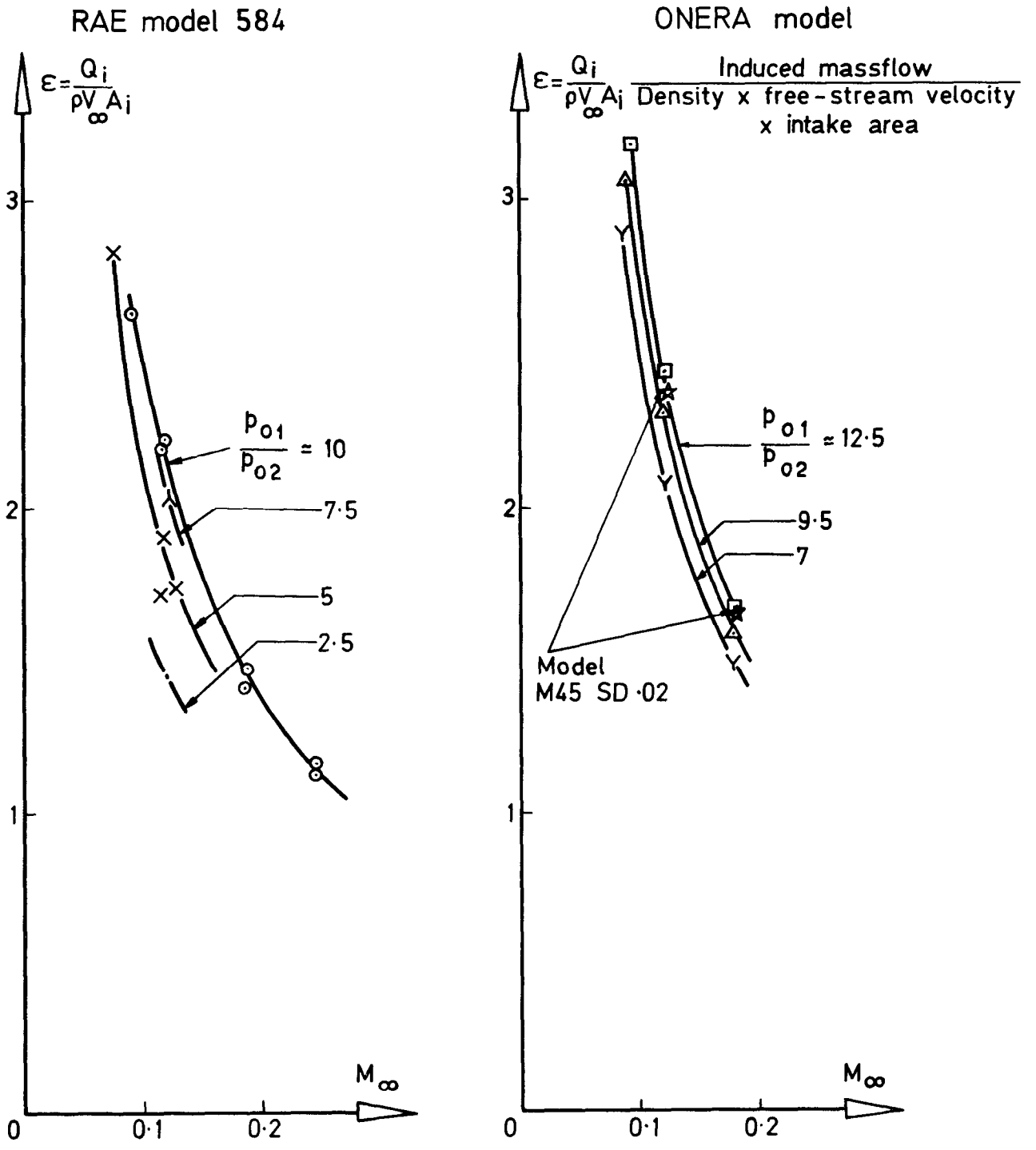

Fig.9 Intake capture coefficient

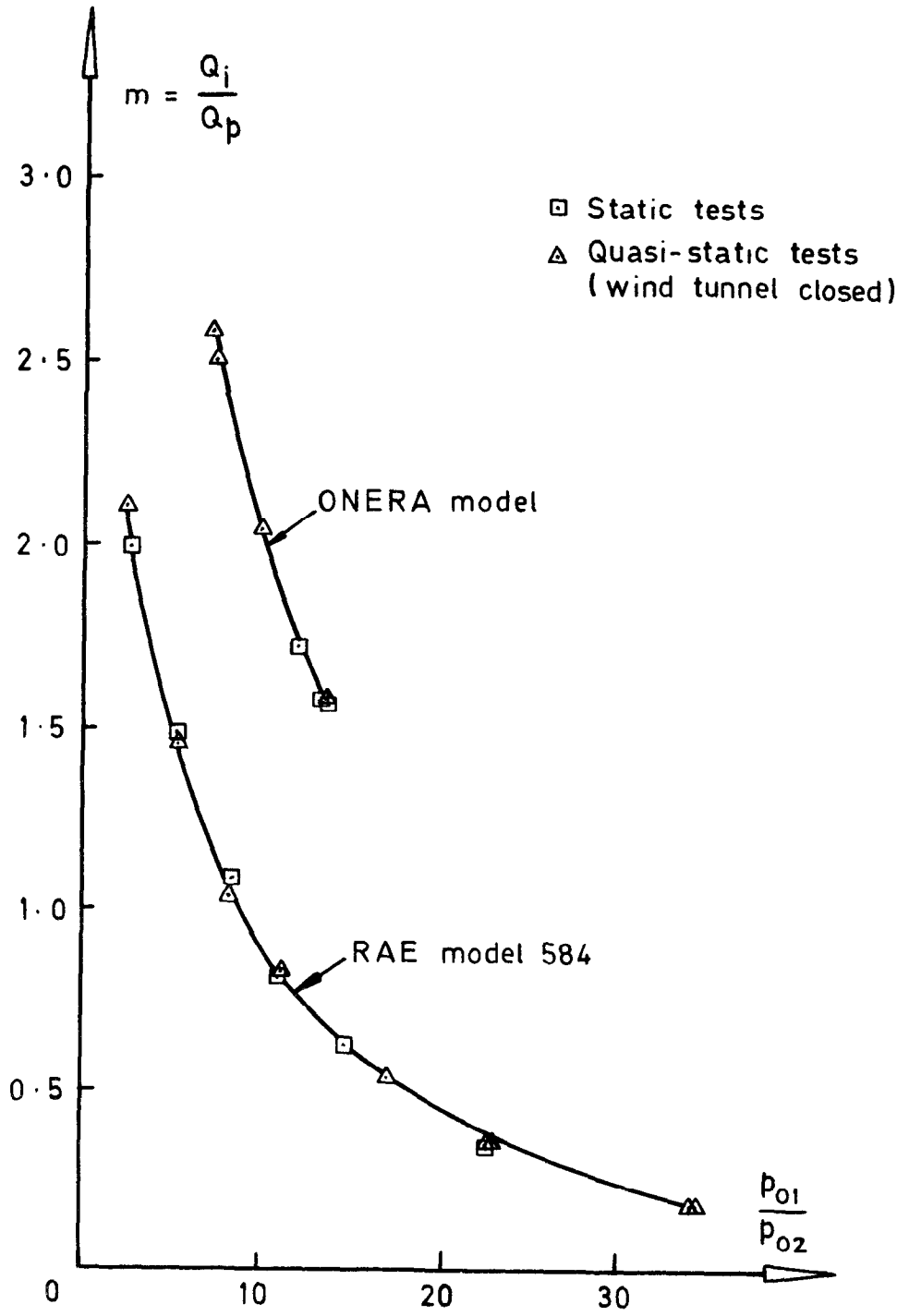

Fig.10 Entrainment coefficient

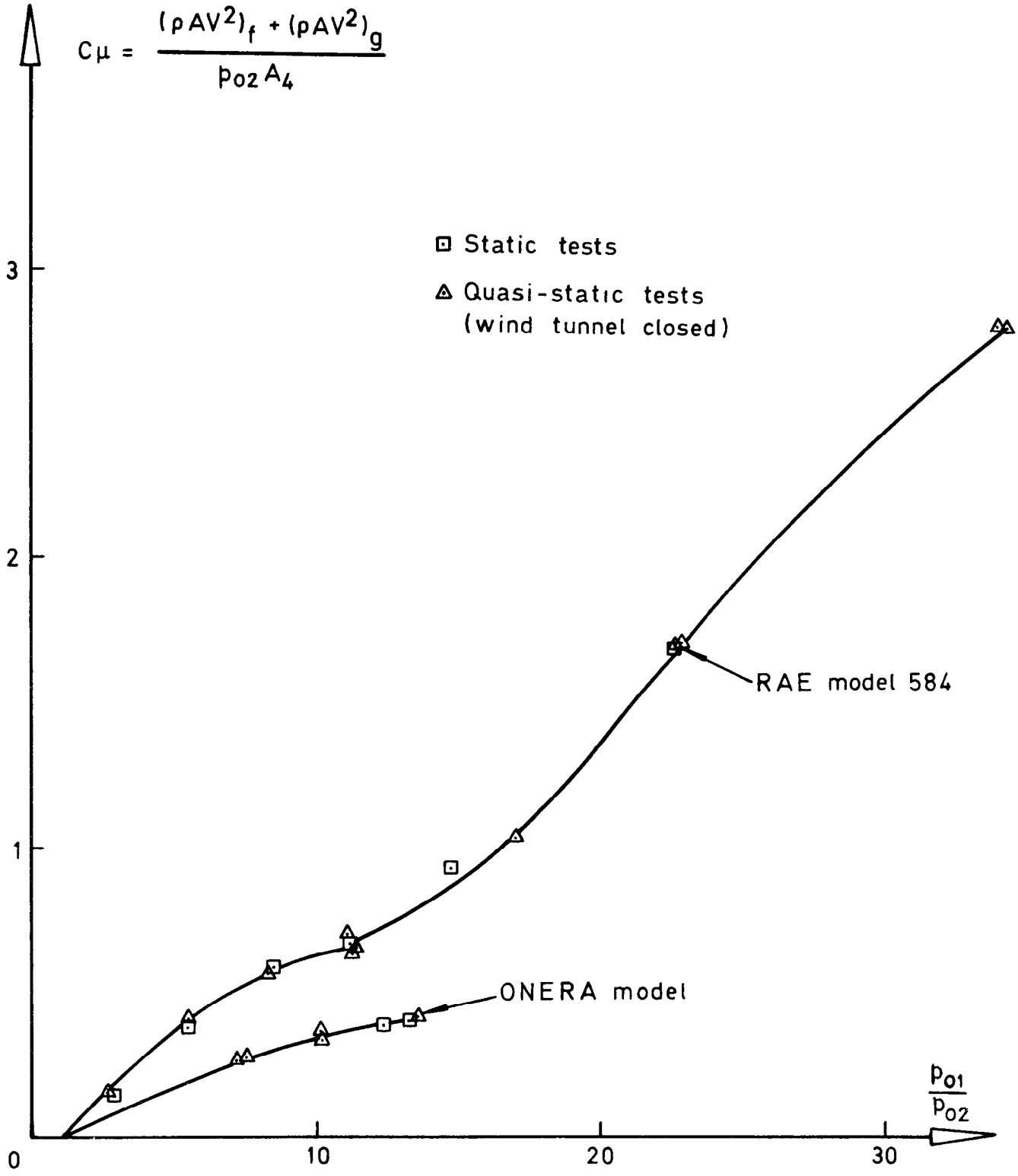

Fig.11 Momentum flow coefficient

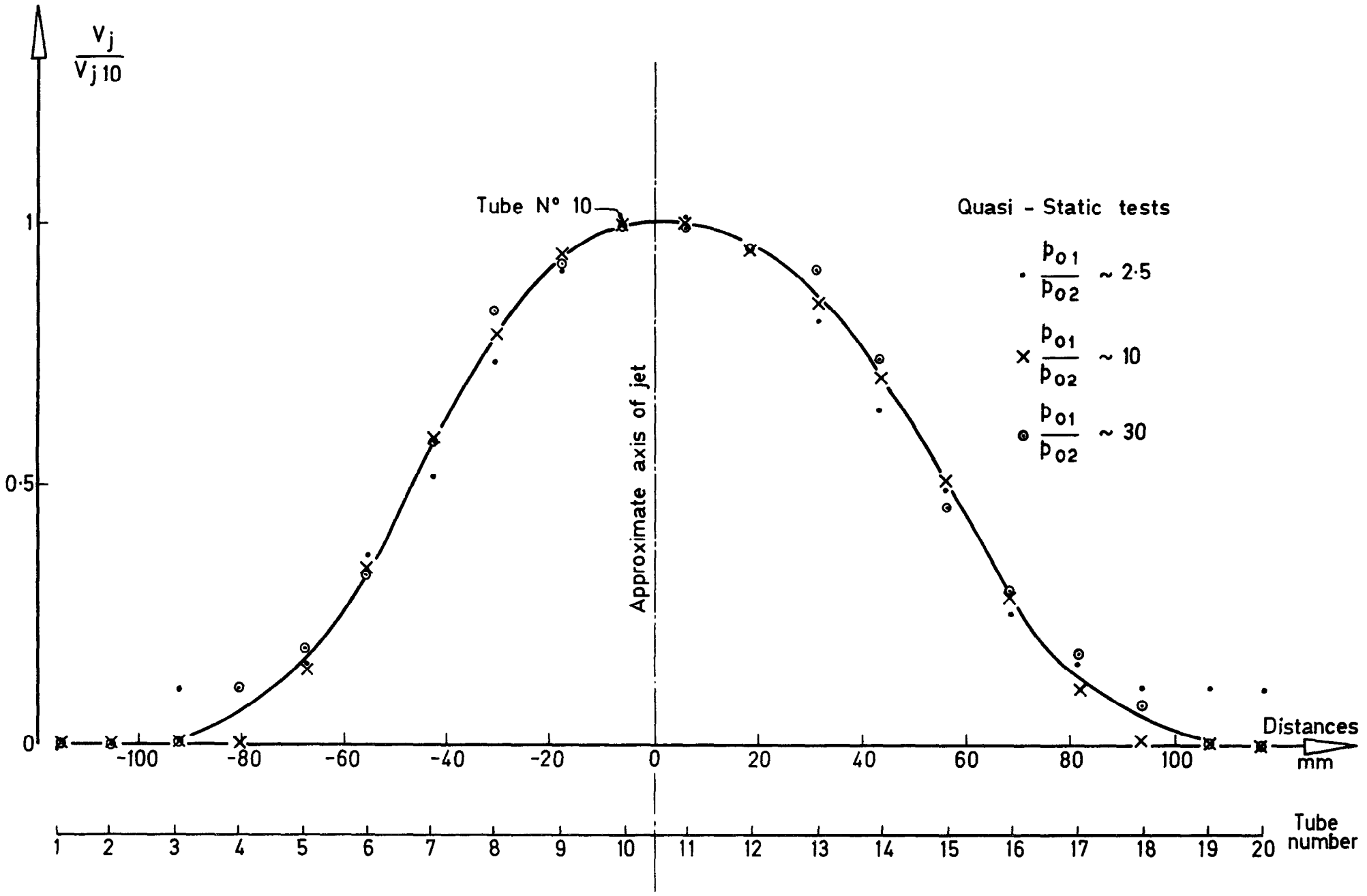

Fig.12 Static velocity distributions in the jet, RAE model 584

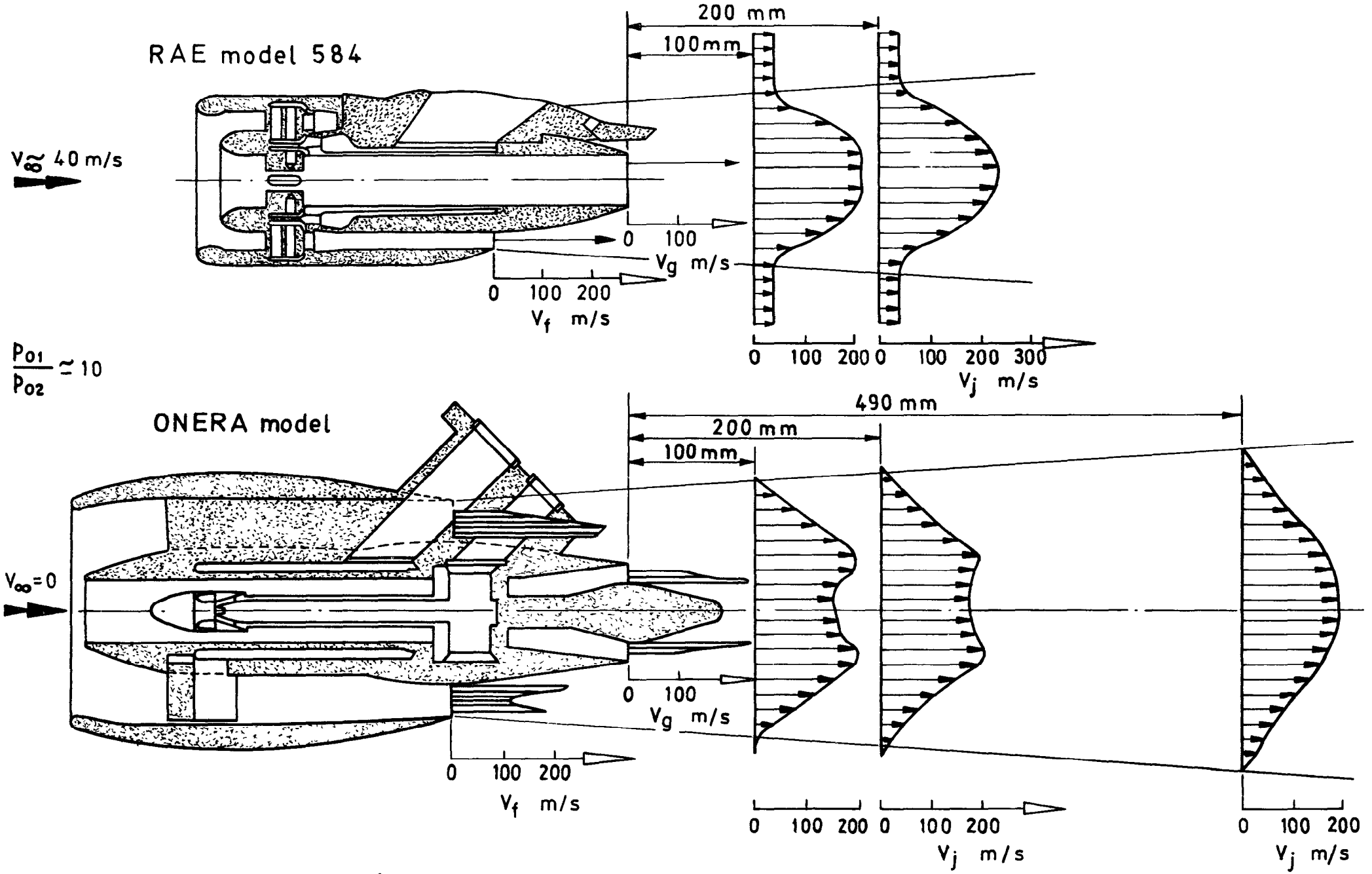

Fig. 13 Velocity profiles in flow downstream of model engines

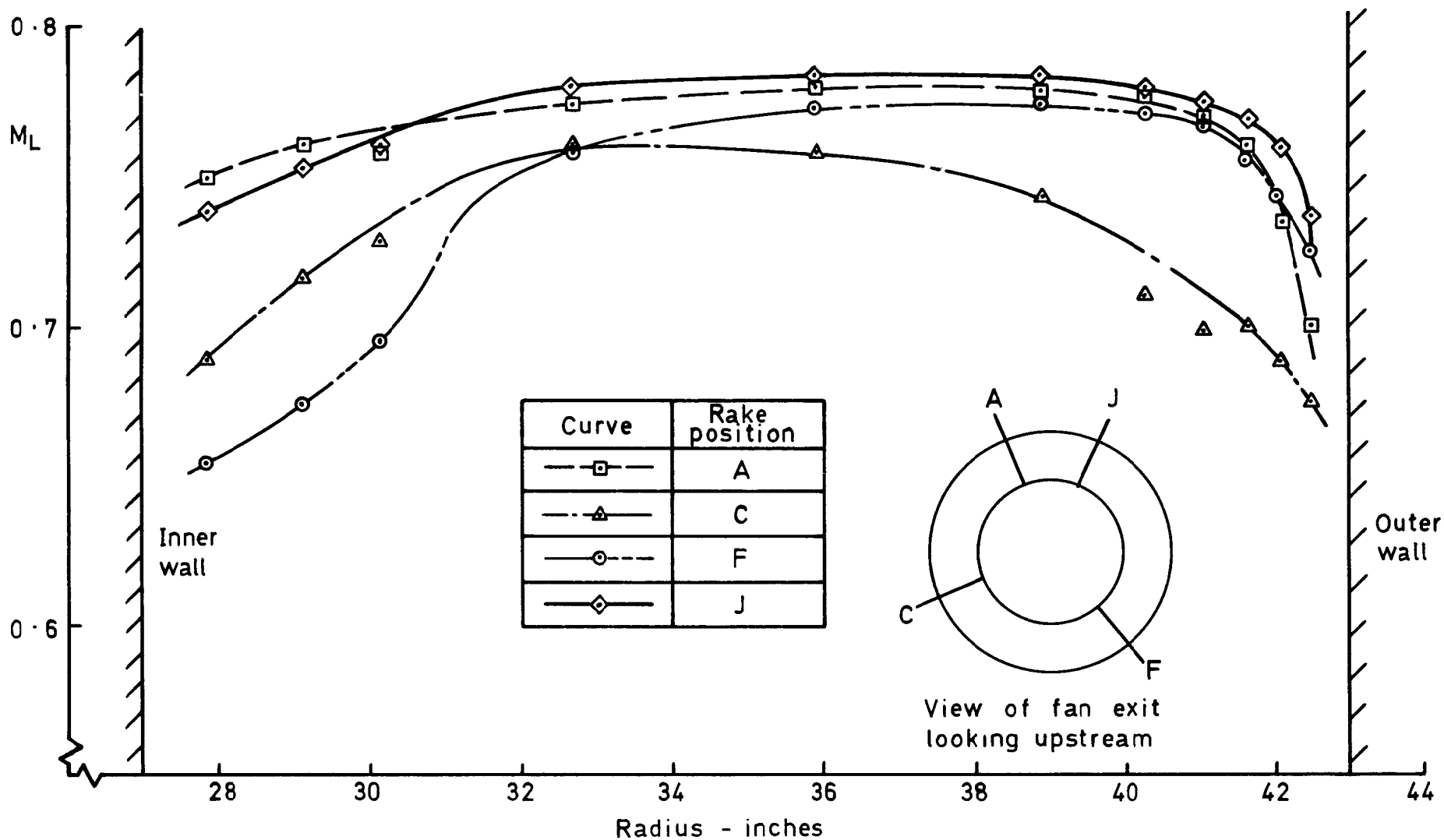

Fig.14 Flow distribution near exit of by-pass duct; RB 211-22; $M_\infty = 0{\cdot}16$

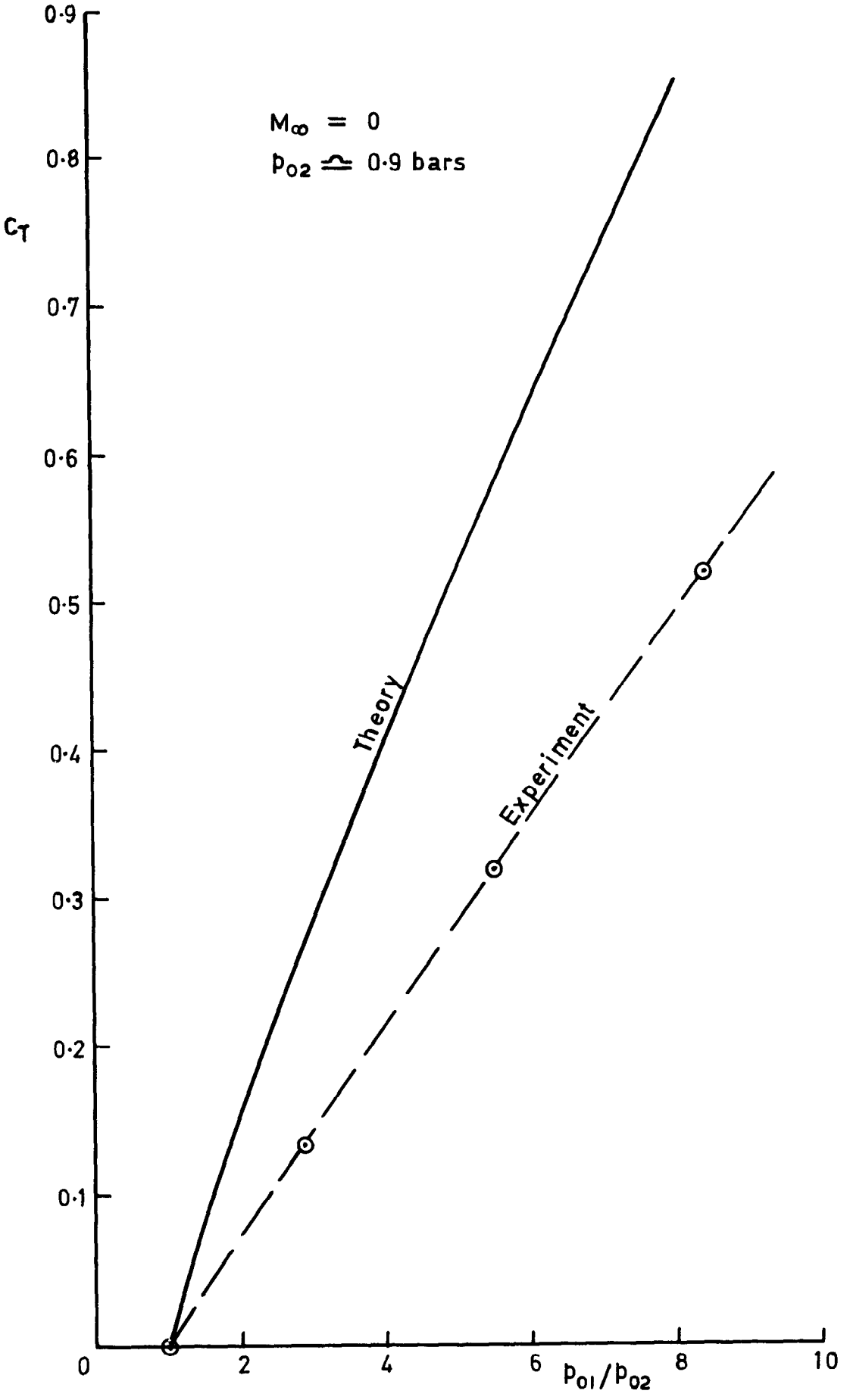

Fig.15 Effect of primary pressure ratio under static conditions. Model 584

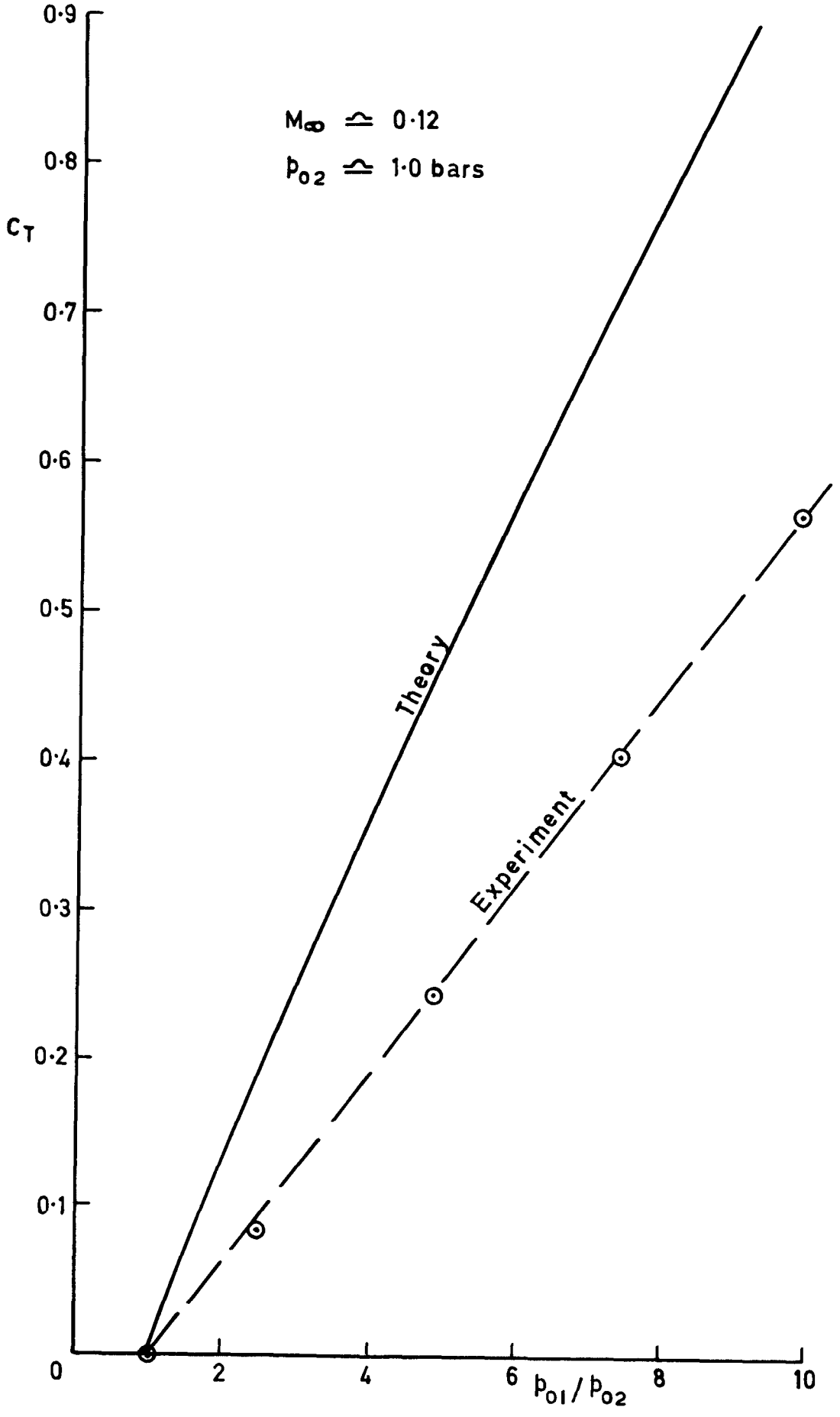

Fig.16 Effect of primary pressure ratio at forward speed. Model 584

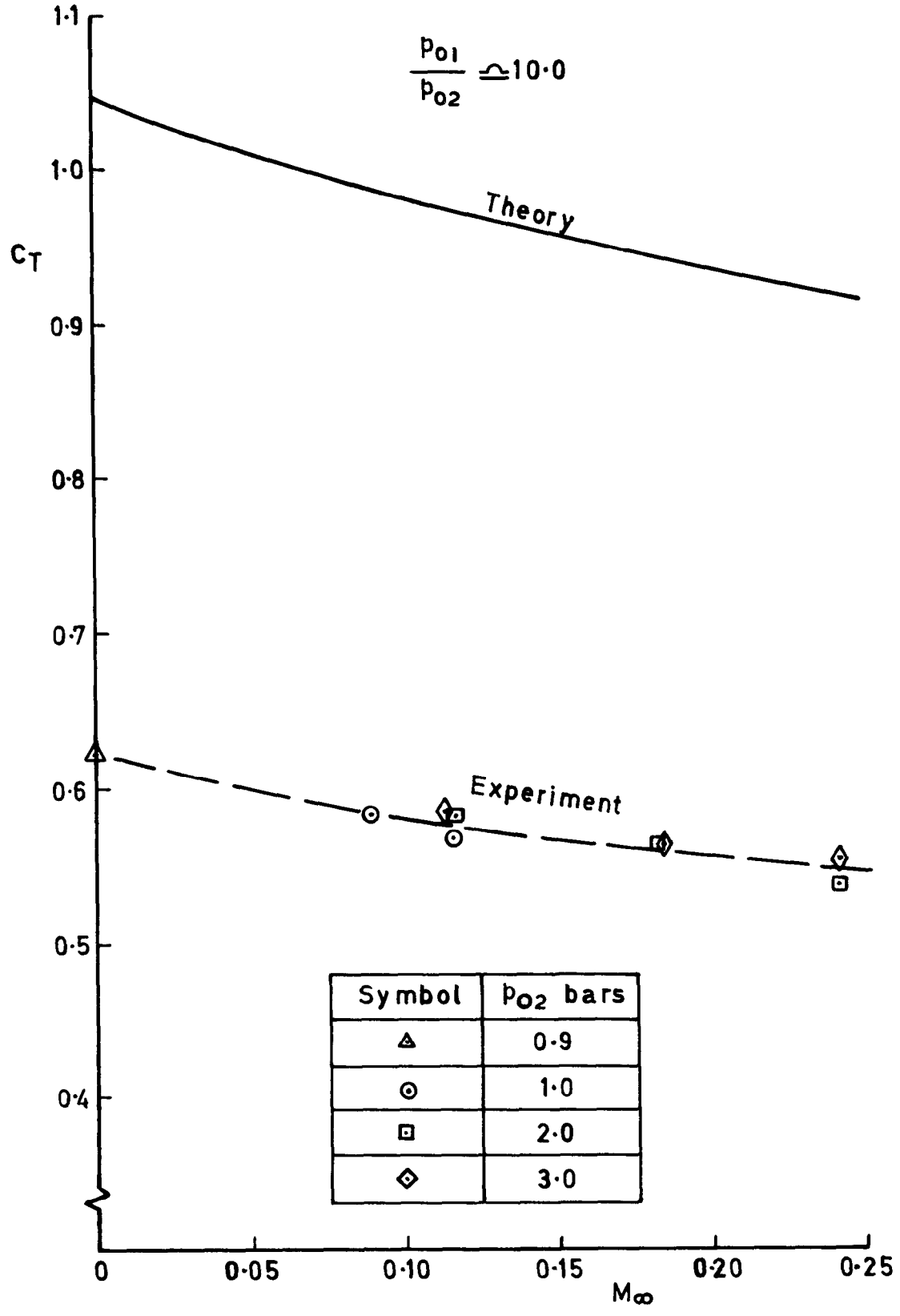

Fig.17 Effect of external pressure on performance of Model 584

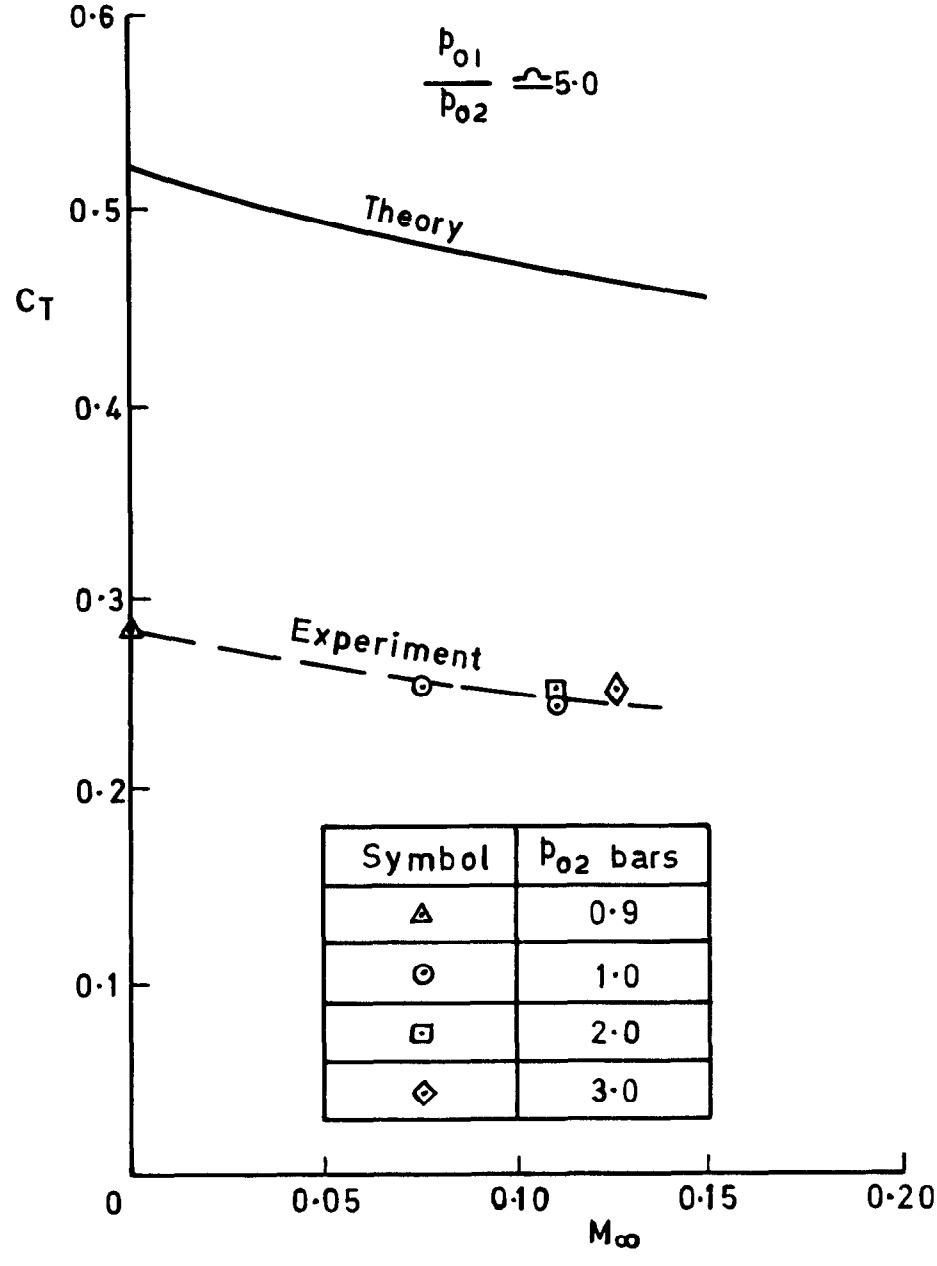

Fig.18 Effect of external pressure on performance of Model 584

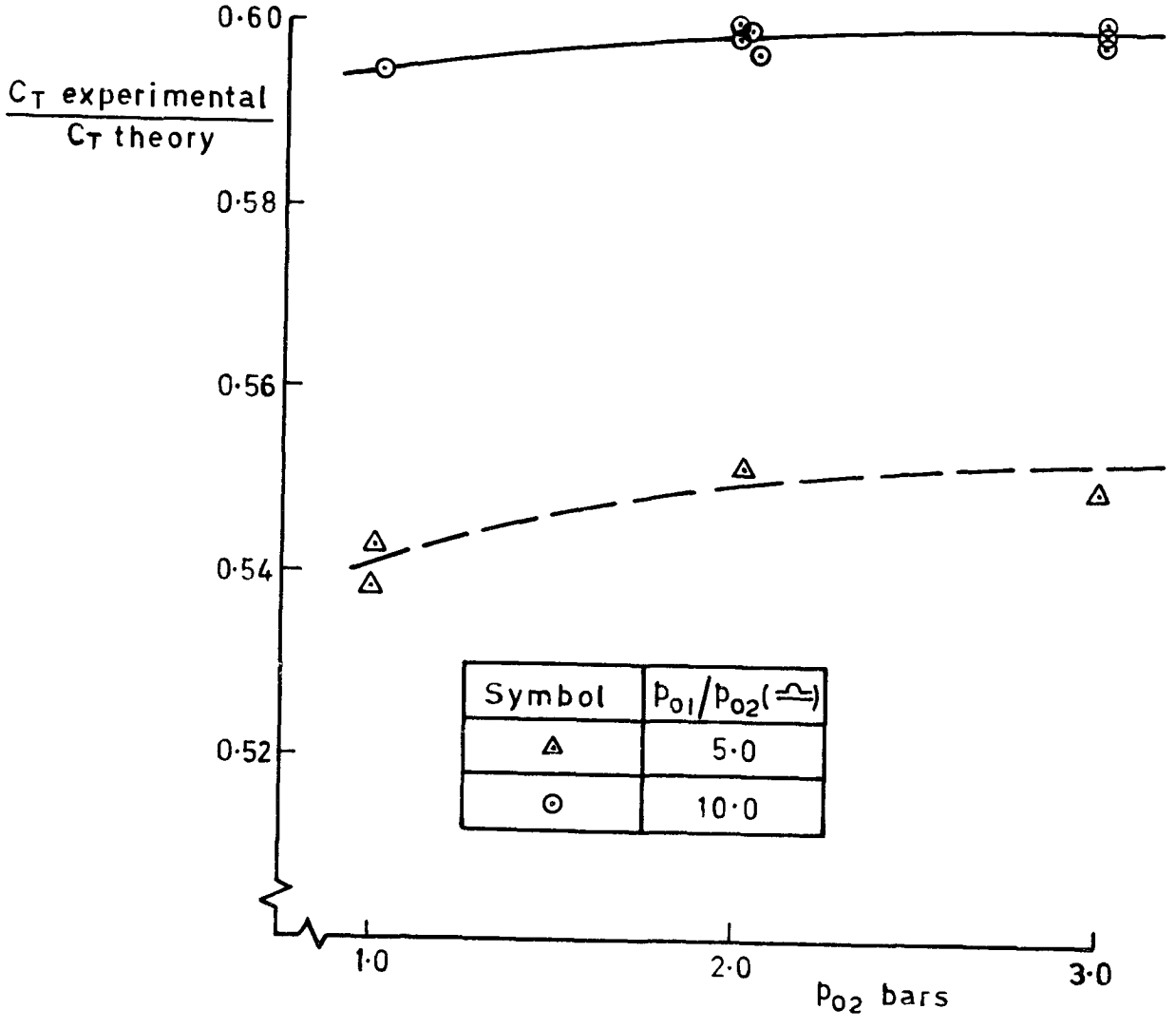

Fig.19 Effect of external pressure on the ratio of experimental thrust coefficient to idealised-injector thrust coefficient. Model 584

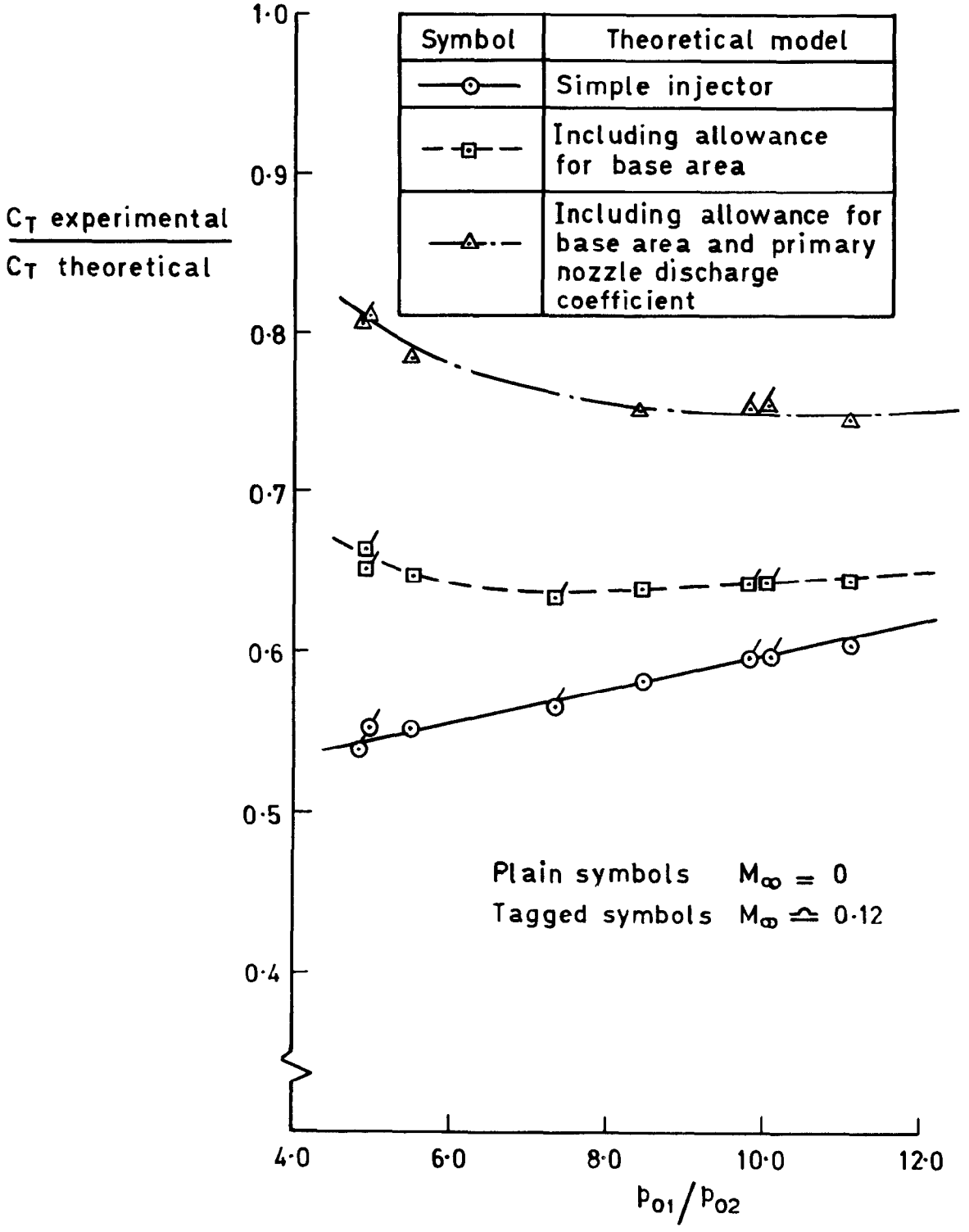

Fig.20 Effect of departures from simplified injector on thrust efficiency of model 584

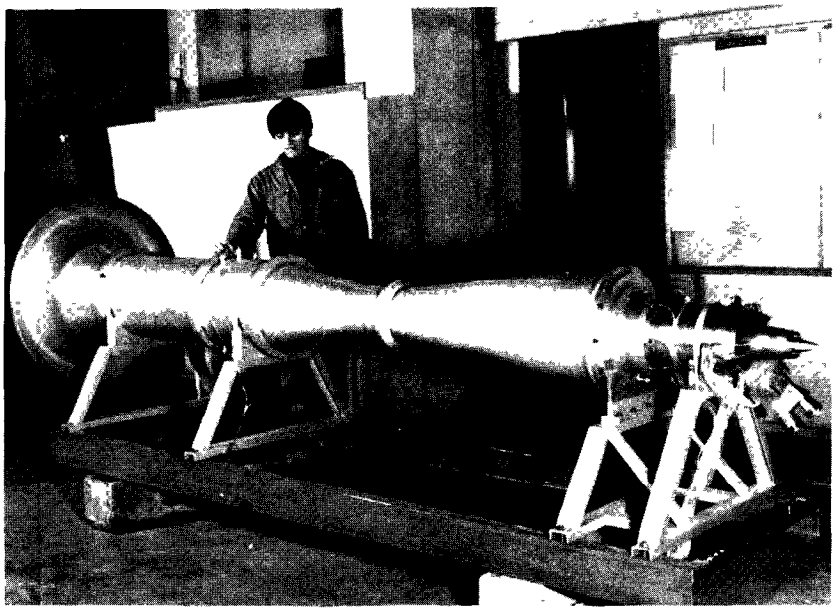

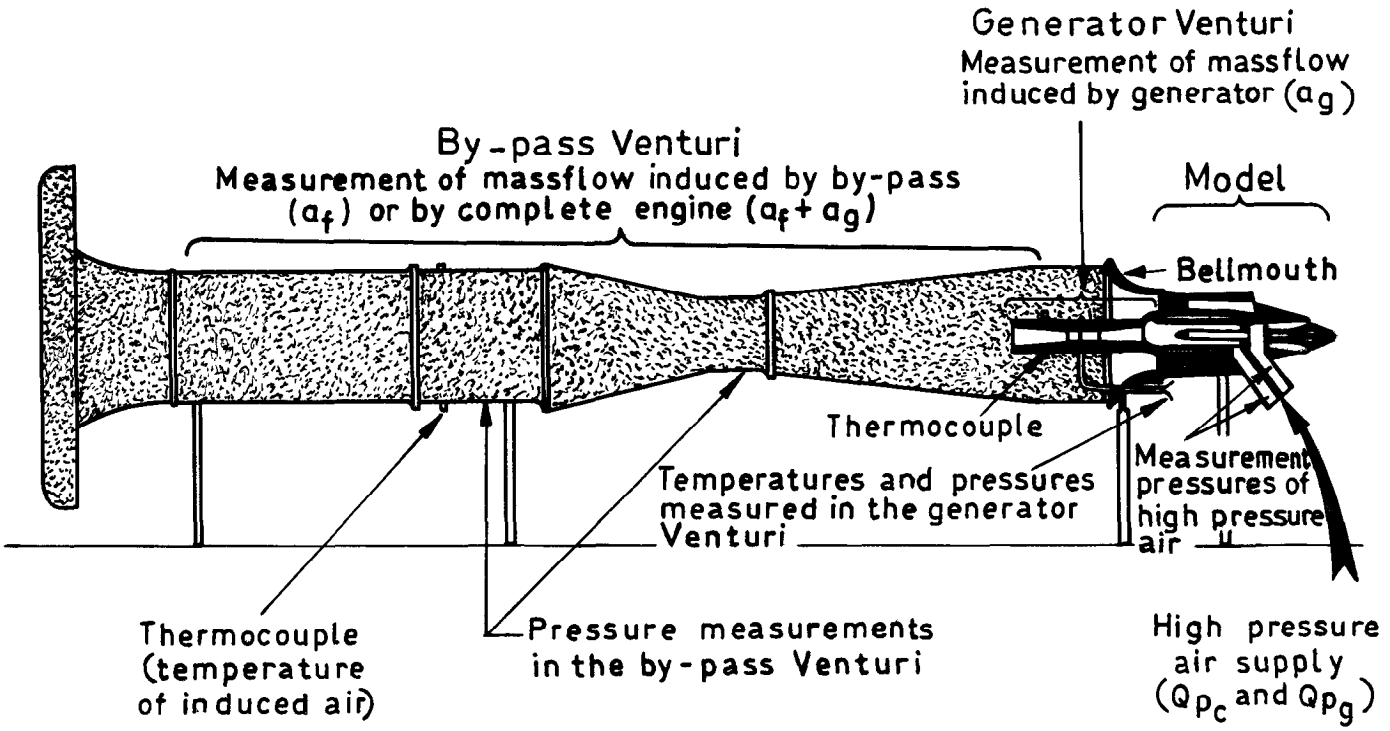

Fig.21 Assembly of rig for static tests

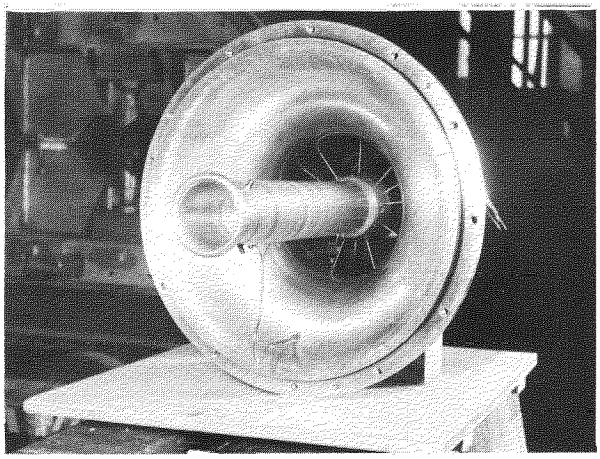

Tests of generator.
Measurement of induced flow by the venturi

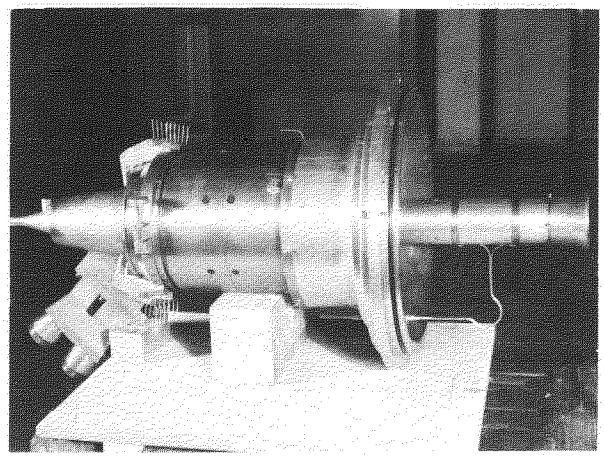

Assembly of engine for
tests of generator

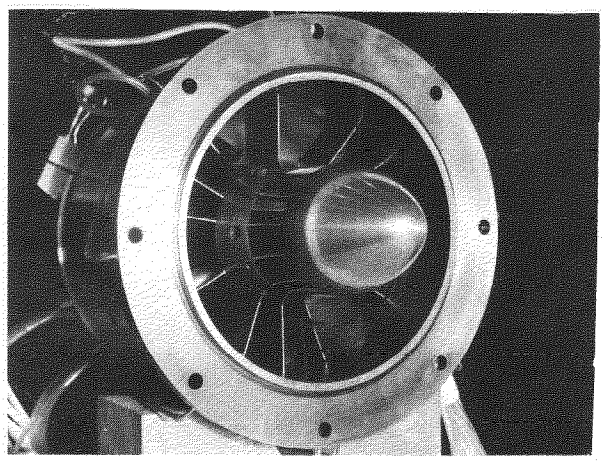

Tests of by-pass
(fairing over intake to generator)

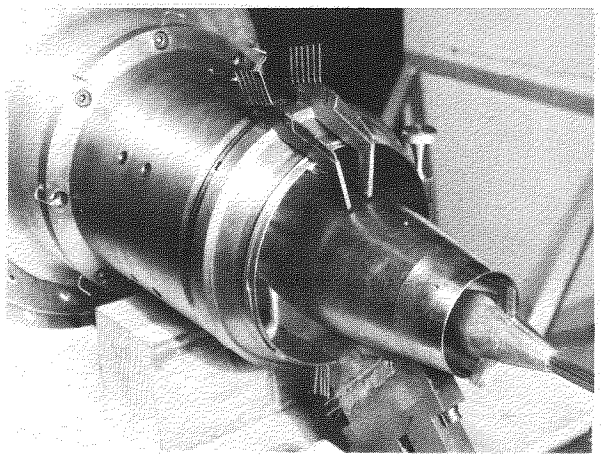

Exit of flows
(rakes at exit of generator and by-pass)

Fig.22 Development of configuration of primary nozzles (details)

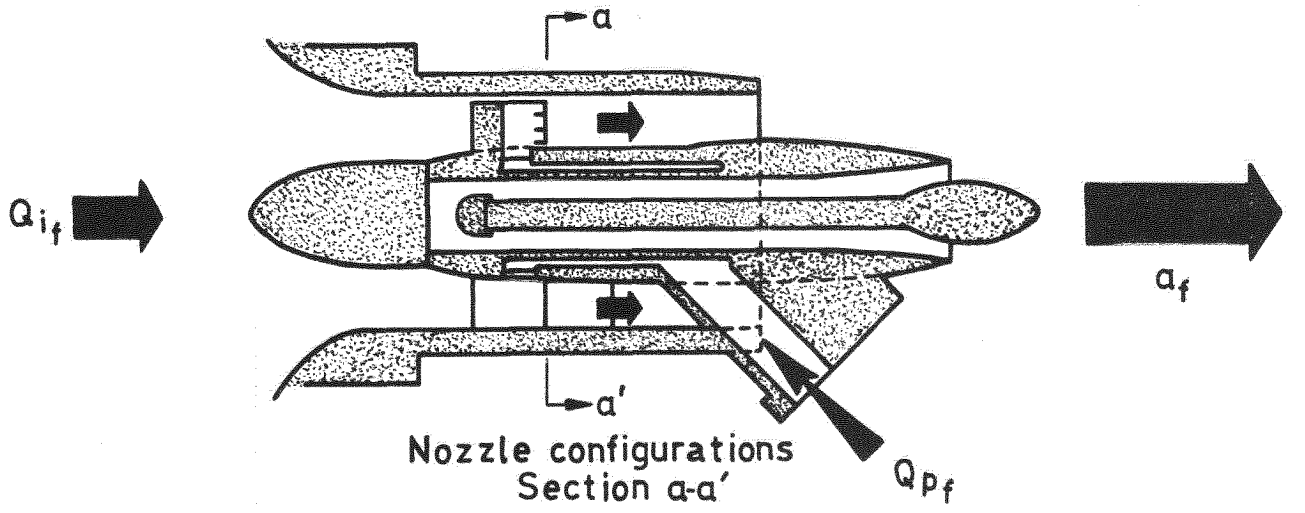

Nozzle configurations
Section a-a'

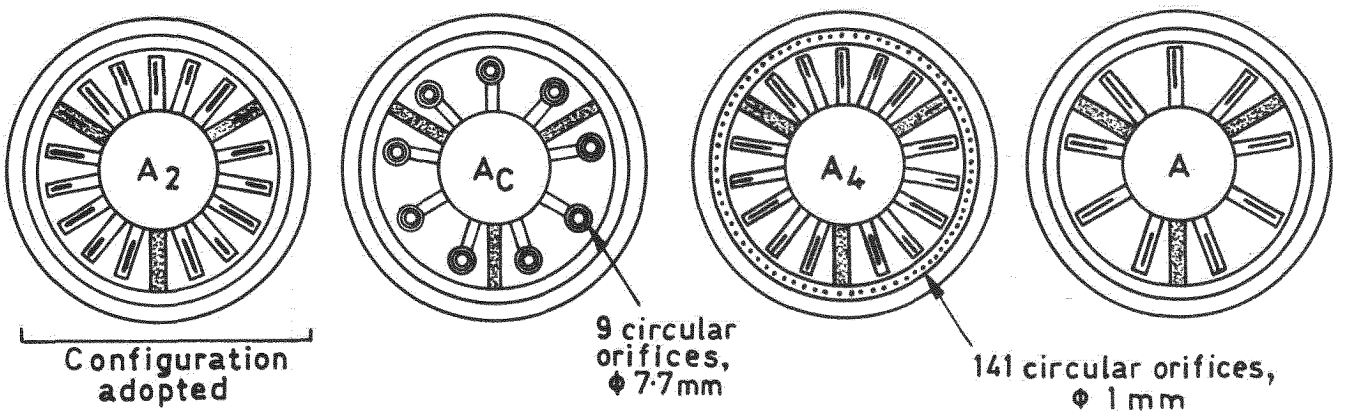

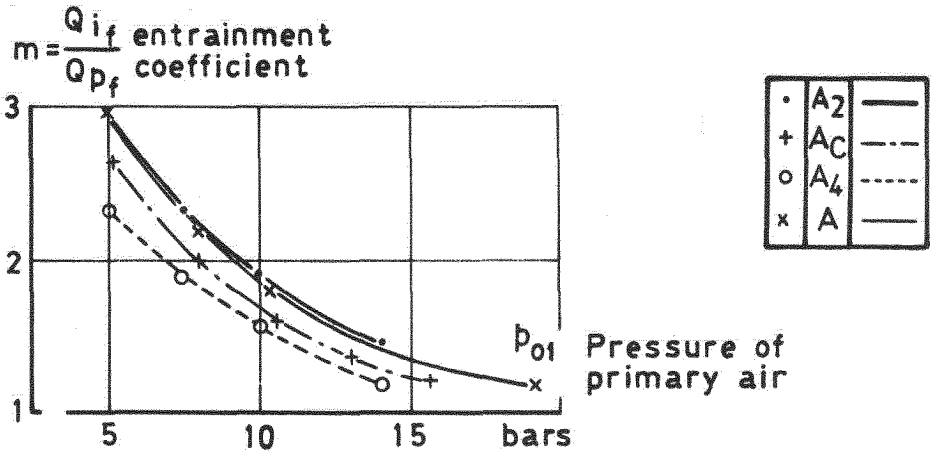

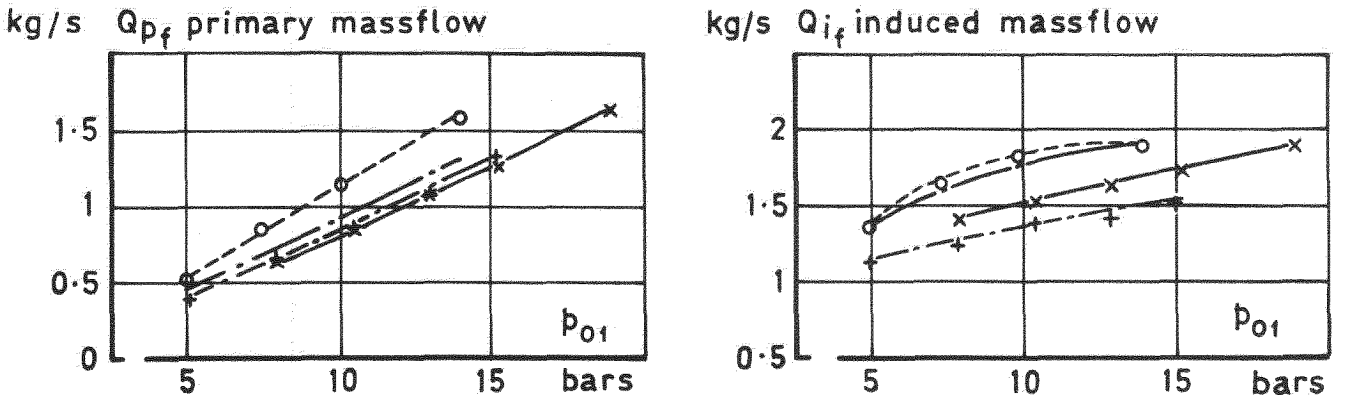

Fig. 23 Development of configuration of nozzles in by-pass

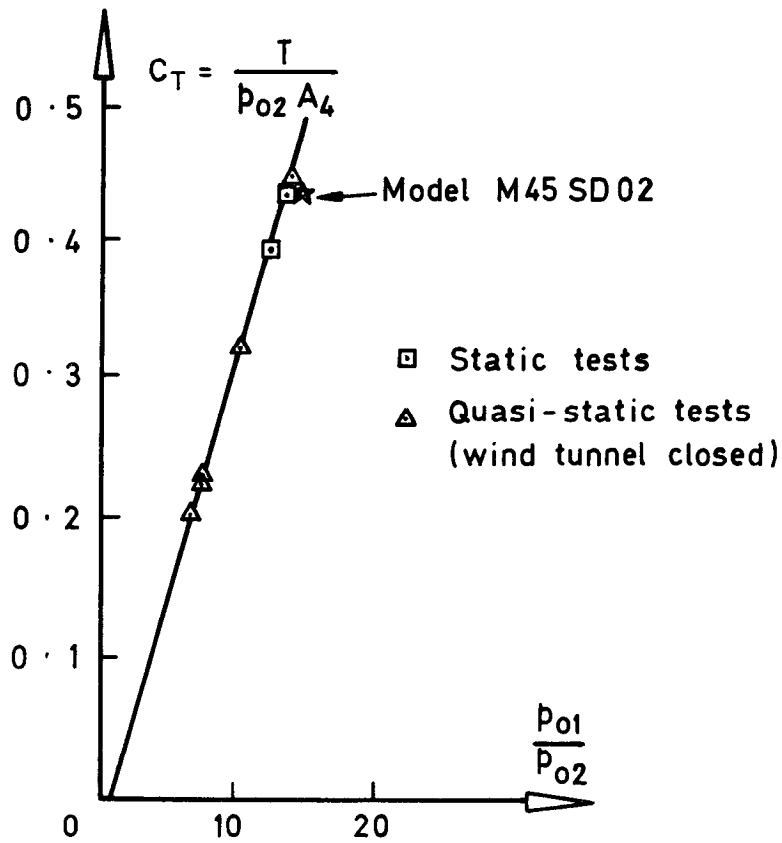

Fig. 24 Static thrust coefficient for ONERA model

Produced in England for Her Majesty's Stationery Office by the Royal Aircraft Establishment, Farnborough. Dd. 587483 K5 6/77.

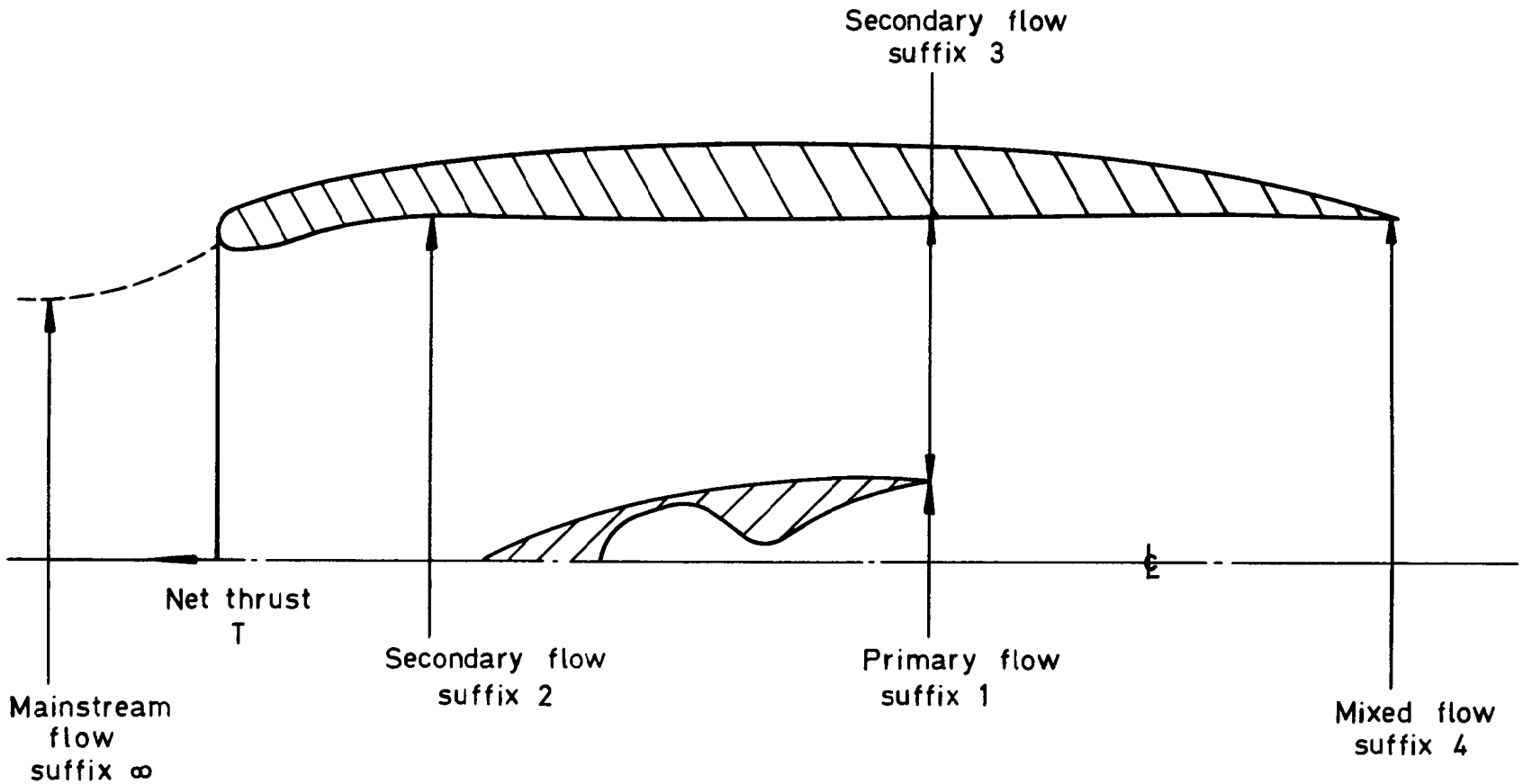

Fig. 25 Simplified injector-powered engine simulation unit, illustrating notation

ARC CP No.1377
February 1976

533.6.072 :
621.438 :
533.6.071.4 :
621.694.2

Masson, A.
Foster, D. N.

THE CALIBRATION OF INJECTOR-POWERED ENGINE SIMULATORS FOR USE IN PRESSURISED WIND TUNNELS

The use of engine simulators based on the injector principle is of interest to both ONERA and RAE for use in their respective low-speed pressurised wind tunnels which are currently under construction. As a result of this common interest, a collaborative programme of work was undertaken within the framework of AFARP 1 (Anglo-French Aeronautical Research Programme).

The possibility of using the S3 wind tunnel at Modane-Avrieux to calibrate injector-powered engine simulators was investigated by ONERA using two engine simulators, one built by ONERA to simulate an engine with a by-pass ratio of 10 (M45S), and one built by RAE to simulate an engine with a by-pass ratio of 5 (RB 211). Tests were carried out over a range of stagnation pressures of both the primary (inducing) flow and of the external

(Over)

ARC CP No.1377
February 1976

533.6.072 :
621.438 :
533.6.071.4 :
621.694.2

Masson, A.
Foster, D. N.

THE CALIBRATION OF INJECTOR-POWERED ENGINE SIMULATORS FOR USE IN PRESSURISED WIND TUNNELS

The use of engine simulators based on the injector principle is of interest to both ONERA and RAE for use in their respective low-speed pressurised wind tunnels which are currently under construction. As a result of this common interest, a collaborative programme of work was undertaken within the framework of AFARP 1 (Anglo-French Aeronautical Research Programme).

The possibility of using the S3 wind tunnel at Modane-Avrieux to calibrate injector-powered engine simulators was investigated by ONERA using two engine simulators; one built by ONERA to simulate an engine with a by-pass ratio of 10 (M45S), and one built by RAE to simulate an engine with a by-pass ratio of 5 (RB 211). Tests were carried out over a range of stagnation pressures of both the primary (inducing) flow and of the external

(Over)

Cut here

ARC CP No.1377
February 1976

533.6.072 :
621.438 :
533.6.071.4 :
621.694.2

Masson, A.
Foster, D. N.

THE CALIBRATION OF INJECTOR-POWERED ENGINE SIMULATORS FOR USE IN PRESSURISED WIND TUNNELS

The use of engine simulators based on the injector principle is of interest to both ONERA and RAE for use in their respective low-speed pressurised wind tunnels which are currently under construction. As a result of this common interest, a collaborative programme of work was undertaken within the framework of AFARP 1 (Anglo-French Aeronautical Research Programme).

The possibility of using the S3 wind tunnel at Modane-Avrieux to calibrate injector-powered engine simulators was investigated by ONERA using two engine simulators; one built by ONERA to simulate an engine with a by-pass ratio of 10 (M45S), and one built by RAE to simulate an engine with a by-pass ratio of 5 (RB 211). Tests were carried out over a range of stagnation pressures of both the primary (inducing) flow and of the external

(Over)

Cut here

DETACHABLE ABSTRACT CARDS

DETACHABLE ABSTRACT CARDS

(induced) flow, under static and low forward speed conditions, with the models at zero angle of incidence. The tests showed that it would be possible to use the S3 wind tunnel to calibrate future engine simulators, and also that, for the conditions tested, the stagnation pressure of the induced flow had only a minimal effect on the non-dimensional performance of the engine simulator.

A description is also given of the tests made in a specially-designed static rig to develop the configuration of the primary nozzles for the ONERA model engine.

(induced) flow, under static and low forward speed conditions, with the models at zero angle of incidence. The tests showed that it would be possible to use the S3 wind tunnel to calibrate future engine simulators, and also that, for the conditions tested, the stagnation pressure of the induced flow had only a minimal effect on the non-dimensional performance of the engine simulator.

A description is also given of the tests made in a specially-designed static rig to develop the configuration of the primary nozzles for the ONERA model engine.

(induced) flow, under static and low forward speed conditions, with the models at zero angle of incidence. The tests showed that it would be possible to use the S3 wind tunnel to calibrate future engine simulators, and also that, for the conditions tested, the stagnation pressure of the induced flow had only a minimal effect on the non-dimensional performance of the engine simulator.

A description is also given of the tests made in a specially-designed static rig to develop the configuration of the primary nozzles for the ONERA model engine.

(induced) flow, under static and low forward speed conditions, with the models at zero angle of incidence. The tests showed that it would be possible to use the S3 wind tunnel to calibrate future engine simulators, and also that, for the conditions tested, the stagnation pressure of the induced flow had only a minimal effect on the non-dimensional performance of the engine simulator.

A description is also given of the tests made in a specially-designed static rig to develop the configuration of the primary nozzles for the ONERA model engine.

Published by
HER MAJESTY'S STATIONERY OFFICE

Government Bookshops
49 High Holborn, London WC1V 6HB
13a Castle Street, Edinburgh EH2 3AR
41 The Hayes, Cardiff CF1 1JW
Brazennose Street, Manchester M60 8AS
Southey House, Wine Street, Bristol BS1 2BQ
258 Broad Street, Birmingham B1 2HE
80 Chichester Street, Belfast BT1 4JY

Government Publications are also available through booksellers

C.P. No. 1377

ISBN 011 471123 2